MACROPHAGE MODULATION BY β-GLUCAN AND RP-182 NANOPARTICLES

EVALUATING THE ABILITY OF β-GLUCAN AND RP-182 DERIVED NANOPARTICLES TO MODULATE MACROPHAGES AS POTENTIAL LUNG FIBROSIS THERAPEUTICS

By: LACHLAN T. MACLEAN, B.Sc.

A Thesis Submitted to the Department of Medical Sciences and the School of Graduate Studies in Partial Fulfillment of the Requirements for the Degree of Master of Science

Master of Science (2025)
(Medical Sciences)

McMaster University
Hamilton, Ontario

TITLE: Evaluating the ability of β-glucan and RP-182 derived nanoparticles to modulate macrophages as potential lung fibrosis therapeutics

AUTHOR: Lachlan T. MacLean

BSc, (Biology)

McMaster University, Hamilton, Ontario

SUPERVISOR: Dr. Dawn Bowdish

NUMBER OF PAGES: xiii, 74

Lay Abstract

Scarring is a process of repairing damage in the body, but excessive scarring can be detrimental. In the lungs, this leads to pulmonary fibrosis, a disease that makes breathing difficult. A type of immune cell called a macrophage normally helps fight infections and heal injuries, but can also cause the harmful scarring in the lungs. Our research tested nanoparticles designed to target these macrophages using specific molecular "keys" that fit certain "locks" or receptors on their surface. We found that β-glucan nanoparticles activated macrophages through the Dectin-1 receptor and altered macrophage function, preventing signals that promote scar formation. In contrast, RP-182 nanoparticles failed to show any effect on macrophages. These results show that successful antifibrotic nanoparticles must target receptors capable of sending signals and have components that are less likely to cause an unintended macrophage response.

Abstract

Pulmonary Fibrosis is a progressive and fatal lung disease characterized by excessive extracellular matrix deposition leading to aberrant thickening and scarring of the lungs. Current therapies include Pirfenidone and Nintedanib, which slow but do not stop disease progression, underscoring the need for new treatment strategies. Macrophages are central regulators of tissue homeostasis, immunity, and repair. In the fibrotic lung, they become aberrantly activated and perpetuate fibrosis by driving fibroblast activation and ECM accumulation. Their high plasticity and receptor diversity make them attractive therapeutic targets for immunomodulatory nanomedicines. We evaluated three nanoparticle platforms designed to modulate macrophage function in the context of pulmonary fibrosis. The first two employed β-glucan, a Dectin-1 agonist with known immunostimulatory activity, formulated as polyelectrolyte complexes and self-assembled nanoparticles. The third utilized RP-182, a synthetic peptide reported to bind to the mannose receptor CD206, conjugated onto a polystyrene nanoparticle. To assess these platforms, bone marrow-derived macrophages were used to understand dose-dependent effects on phenotype and uptake. Precision-cut lung slices provided a multicellular *ex vivo* approach to assess gene expression through RT-qPCR. β-glucan nanoparticles, especially the self-assembled platform, induced a shift in BMDM phenotype toward pro-inflammatory, increasing surface expression of MHCII and CCR2 and transcription of *Tnf* in our PCLS model. In contrast, RP-182 conjugated nanoparticles failed to alter macrophage phenotype, where the increase in pro-inflammatory markers and preferential nanoparticle uptake observed were a result of the polystyrene vehicle. These findings demonstrate that ligand choice and nanoparticle composition critically shape macrophage response. Overall, this work emphasizes the need to couple effective

ligand choice with biocompatible carriers to target macrophages and mitigate fibrosis progression.

Acknowledgments

I would like to begin by expressing my gratitude to my supervisor, Dr. Dawn Bowdish. Her guidance and unwavering support were nothing short of essential in my success as a graduate student.

To my fellow lab members, I could not have done it without you all. You made the late nights and long days in the lab bearable, some might even say enjoyable. As my time as part of the Bowdish Lab comes to an end, you all are what I will miss the most.

To Dr. Andrew Thompson, Dr. Joanna Wilson, and most importantly, Dr. Andrea Murillo, I would not be here without you. You took a chance on a wide-eyed undergrad, which inevitably brought me to where I am today. You fostered my love for science and pushed me to reach higher, so thank you.

To my partner, Izabella, you believed in me when I didn't believe in myself. You were there for every phone call, text, and conversation. You lived my excitement and my disappointment. You lifted me up when I needed you to, and you were by my side the whole way. There are not enough words to express my appreciation for all that you have helped me achieve, so you'll have to settle for a 'thank you'.

Lastly, to my parents, David and Michelle, and my brothers, Chance and Aiden, I would not be who I am or where I am without your continued love and support. Other things may change us, but we start and end with family. Virtue Mine Honour.

Table of Contents

List of Figures

List of Tables

Abbreviations

α-SMA	Alpha-smooth muscle actin
BMDM	Bone marrow-derived macrophage
CD	Cluster of differentiation
CCR2	C-C chemokine receptor type 2
cDNA	Complementary DNA
DTT	Dithiothreitol
ECM	Extracellular matrix
FGF	Fibroblast growth factor
HDAC3	Histone deacetylase 3
IFNγ	Interferon gamma
IgG	Immunoglobulin G
IM	Interstitial macrophages
IL	Interleukin
iNOS	Inducible nitric oxide synthase
LPS	Lipopolysaccharide
MAPK	Mitogen-activated protein kinase
MHCII	Major histocompatibility complex class II
MoAM	Monocyte-derived alveolar macrophage
NF-κB	Nuclear factor kappa-light-chain-enhancer of activated B cells
PBS	Phosphate-buffered saline
PDGF	Platelet-derived growth factor
PEC	Polyelectrolyte complex (nanoparticle)
PCLS	Precision-cut lung slices
PF	Pulmonary fibrosis
PPAR	Peroxisome proliferator-activated receptor
PS	Polystyrene
qPCR / RT-qPCR	Quantitative polymerase chain reaction / Reverse transcription quantitative polymerase chain reaction
ROS	Reactive oxygen species
SA	Self-assembled (nanoparticle)
STAT	Signal transducer and activator of transcription
TGFβ	Transforming growth factor beta
Th2	T-helper type 2
TIMPs	Tissue inhibitors of matrix metalloproteinases
TRAM	Tissue-resident alveolar macrophage
VEGF	Vascular endothelial growth factor
WT	Wild type
ILD	Interstitial Lung Disease
ATP	Adenine triphosphate

TLR	Toll-like receptor
TNF	Tumour necrosis factor
FITC	Fluorescein isothiocyanate
RNA	Ribonucleic acid
R10	RPMI supplemented with 10% Fetal bovine serum
FBS	Fetal bovine serum
SEM	Standard error of the mean
JAK	Janus kinase
POLAMA	Poly(oligo(lactic acid) methacrylate)
DOX	Doxorubucin
gMFI	Geometric mean fluorescent intensity
POEGMA	Poly(oligo(ethylene glycol) methyl ether methacrylate)

Declaration of Academic Achievement

This thesis is the summary of the research I completed throughout the last two years as a Master's candidate. This thesis was written entirely by myself, with editing input from Dr. Dawn Bowdish as well as Dr. Jessica Breznik. All experiments, data collection, data analysis, and data visualization were performed and completed by me.

All nanoparticle materials used in this thesis were supplied by our collaborators. Nate Dowdall from Dr. Todd Hoare's Lab supplied all β-glucan materials. All RP-182 related materials were supplied by Chuan Yu from Dr. Ryan Wylie's Lab. Additionally, biolayer interferometry and related data collection, analysis, and visualization were done by Chuan Yu.

Chapter 1: Introduction

1.1 Lung Fibrosis – A Brief Overview

Fibrosis is defined as the hardening and scarring of tissues caused by the accumulation of extracellular matrix (ECM) components such as collagen and fibronectin. It is often the end-stage manifestation of diseases such as Interstitial Lung Disease (ILD) (T. Wynn, 2008). ILD is a term that represents a group of parenchymal lung disorders associated with high morbidity and mortality (Antoniou et al., 2014). These conditions are characterized by chronic lung inflammation and fibrosis, accumulation of immune cells, increased levels of cytokines, and chemokines (Kalchiem-Dekel et al., 2018). Patients with ILD often develop progressive fibrosis of the lungs called pulmonary fibrosis (PF). Currently, it is understood that PF arises from aberrant scarring and thickening of the lung interstitium. This thickening and scarring increases the thickness of the interstitial space and decreases the mechanical capacity of the lungs to expand and contract, decreasing gas exchange. The inability for adequate oxygen to enter the bloodstream and difficulty of breath eventually leads to respiratory failure and subsequently death (Koudstaal et al., 2023; Wijsenbeek et al., 2022). Unfortunately, there is still very little that is known about the etiology of PF, and there are very few treatment options to combat its progression. Therefore, new insights and therapeutics are urgently required.

1.2 The Role of Fibroblasts and Myofibroblasts in Lung Fibrosis

Fibroblasts are the workhorse of the body, maintaining a heterogeneous array of ECM-rich connective tissues, providing niches and positional information to neighbouring cells (Plikus et al., 2021). The most important role they play is maintaining tissue homeostasis following an abrasion or injury through the process of tissue regeneration. Fibroblasts are mesenchymal cells,

a population of stromal cells that originate from the mesenchyme and contribute to tissue structure and repair, with self-renewal properties. They are heavily implicated in the onset and progression of PF through the development of a specialized microenvironment that promotes excessive ECM accumulation, often referred to as the 'fibrotic niche' (Herrera et al., 2018). Currently, there is speculation as to how fibroblasts perpetuate fibrosis through several potential sources of expansion within the fibrotic lung. Three hypotheses are presented to explain their source. The first being that they originate from resident fibroblasts. The second describes their recruitment and subsequent differentiation from bone marrow progenitors. The third is that they are derived from alveolar epithelial cells through epithelial to mesenchymal transition (Yamaguchi et al., 2017). Regardless of their source, these fibroblasts can eventually become activated biochemically or mechanically. Biochemically, myofibroblast activation is primarily driven by TGFβ signalling through SMAD-dependent and non-canonical pathways, alongside other cytokines and growth factors. Mechanically, increasing ECM stiffness during wound repair provides the tension cues that promote fibroblast transition into α-smooth muscle actin (α-SMA) positive myofibroblasts, establishing a positive feedback loop where contractile activity further stiffens the ECM and sustains myofibroblast activation (Younesi et al., 2024). Upon activation, myofibroblasts produce high levels of ECM components such as collagen, laminin, and fibronectin, contributing heavily to increased scar tissue accumulation when they persist within tissue for an extended period of time (Doolin et al., 2021; Kendall & Feghali-Bostwick, 2014). Myofibroblasts are characterized by increased contractile ability as well as expression of α-SMA (Midgley et al., 2013). Together, fibroblasts and myofibroblasts create fibroblastic foci, which describe areas of heavy tissue remodelling and fibrous tissue buildup commonly found within the PF lung (Tanabe et al., 2020).

1.3 Current Treatments for Lung Fibrosis

Fibrotic disease remains poorly understood, and as a result, options for those with lung fibrosis are limited to lung transplantation for end-stage patients who present specific clinical characteristics. Until recently, lung transplantation was the only option for end-stage patients with PF; however, there are two antifibrotic therapeutics approved by the FDA in 2014 to treat PF and other fibrotic diseases (Dempsey et al., 2021).

Pirfenidone, an orally ingested antifibrotic and anti-inflammatory medication used to treat PF, was approved for use in Japan in 2008 (Ikeda et al., 2022; Lancaster et al., 2017). Pirfenidone slows lung fibrosis progression with limited adverse effects and is supported by data from phase II and phase III clinical trials showing both safety and efficacy in patients with PF (Lancaster et al., 2017). As a small molecule inhibitor, Pirfenidone acts to reduce fibroblast proliferation, migration, and myofibroblast differentiation (Hall et al., 2018). More specifically, it acts on the TGFβ signalling pathway, inhibiting phosphorylation of SMAD 2/3 and p38 MAPK (Aimo et al., 2022; Kolosova et al., 2011). Through this inhibition, downstream expression of fibronectin and collagen I, key factors involved in the development of lung fibrosis, are significantly reduced (Kolosova et al., 2011; Wight & Potter-Perigo, 2011).

The second of the two antifibrotic therapeutics is Nintedanib. Originally developed for the treatment of cancer (Vancheri, 2015), it was adopted for the treatment of PF. Nintedanib works to slow fibrosis progression through binding of the intracellular ATP-binding pocket of various tyrosine kinases of fibroblasts, such as platelet-derived growth factor receptors (PDGFRs), and vascular endothelial growth factor receptors (VEGFRs) (Wollin et al., 2015). By binding to these kinases, Nintedanib represses autophosphorylation of the receptors, preventing the induction of a signalling cascade (Wollin et al., 2015). The loss of this signalling cascade thus

results in decreased fibroblast proliferation, differentiation, and motility within the fibrotic lung (Wollin et al., 2019). In clinical trials, Nintedanib has been shown to decrease the rate of lung function decline as well as the incidence of acute exacerbations (Richeldi et al., 2011). In addition, minimal notable side effects were reported with a discontinuation rate of less than 5% suggesting Nintedanib alone is a relatively safe therapeutic to slow fibrosis progression in the lungs (Richeldi et al., 2014).

Separately, both Pirfenidone and Nintedanib monotherapy decrease the rate of PF progression with minimal side effects, but counterintuitively, combining them does not further slow the course of disease (Flaherty et al., 2018). Neither of these therapeutics are curative, and the only treatment shown to significantly increase median survival time is lung transplantation (Balestro et al., 2019). Like any organ transplant, there is a limited organ donor supply, and unfortunately, PF patients still have the lowest post-transplantation survival time among all lung transplant patients (Kistler et al., 2014). Therefore, the need for therapeutics that halt fibrosis progression and result in minimal side effects is a priority in the treatment of PF.

1.4 Macrophage Populations of the Lung

Macrophages contribute to growth, development, and homeostasis, as well as tissue repair and regeneration (T. A. Wynn et al., 2013), but when those functions are disrupted, they drive the onset and progression of various conditions such as autoimmune, cancer, and chronic inflammatory diseases (Bowdish & Gordon, 2009). In the past two decades, scientists have garnered a better understanding of the disease and the role that macrophages play in PF pathology.

Within the lung, there are two distinct populations of macrophages. The first population, called interstitial macrophages (IM), originate from the yolk sac and seeds the lungs during late embryogenesis and resides in the interstitial space within the lungs, namely the alveolar septa (Hume et al., 2020). Much is to be elucidated regarding IMs and their role in PF or disease in general due to the difficult and strenuous methodology required to extract them from the lung (Liegeois et al., 2018). The second of the two populations is tissue-resident alveolar macrophages (TRAMs). TRAMs are also embryonically derived and are localized in the distal lung on the luminal surface of the alveolar space (Malainou et al., 2023). TRAMs act as the primary phagocytes within the lung and have the job of clearing alveolar surfactant (T'Jonck et al., 2018). In addition, TRAMs ingest allergens, toxic particles, or infectious agents to maintain homeostatic balance (N. Joshi et al., 2018; Rubins, 2003).

Under homeostatic conditions, the macrophage population within the lung contains a greater number of TRAMs than other macrophage subsets (McQuattie-Pimentel et al., 2018). Upon injury or infection, TRAMs are depleted and circulating monocytes or monocytes from precursors in the bone marrow are recruited to the lung to reconstitute this loss (Goto et al., 2004; Misharin et al., 2013). After leaving circulation, these monocytes migrate towards areas of inflammation in a CCR2-dependent manner and become known as monocyte-derived alveolar macrophages (MoAMs) (McQuattie-Pimentel et al., 2018; Shi & Pamer, 2011).

1.5 Macrophage Polarization

The macrophage population in the lung is one of great heterogeneity, and these differences become even more amplified in response to epithelial injury. As mentioned, in the steady state, the lung consists of IM and TRAM macrophage populations with the addition of MoAMs under defence conditions. Macrophages from all three populations undergo a process called polarization/activation induced by specific environmental cues within their respective microenvironments. It is important to note that macrophage phenotype cannot be properly defined, and their profiles are very much a spectrum that is constantly changing. Historically, the terms M1 (classically activated) or M2 (alternatively activated) have been used to categorize macrophage polarization. However, this dichotomy is inaccurate and fails to account for the differences in ontogeny, function, species, and widely underscores their heterogeneity and plasticity.

Inactivated macrophages become polarized to the pro-inflammatory phenotype through stimulation by lipopolysaccharide (LPS) and IFNγ (Mantovani et al., 2013). Pro-inflammatory activation is regulated by signalling pathways STAT1, IRF5, IRF3, and NF-κB (Porta et al., 2015). The result of the signalling cascade is the expression of specific markers and pro-inflammatory molecules. Pro-inflammatory macrophage activation markers include inducible nitric oxide synthase (iNOS), major histocompatibility complex (MHCII), Toll-like receptor 2 (TLR-2), TLR-4, CD80, and CD86 (Perrot et al., 2023). Pro-inflammatory molecules released by these activated macrophages include TNF, IL-1α, IL-1β, IL-6, IL-8, and IL-12 (Arango Duque & Descoteaux, 2014). Epigenetic mechanisms such as histone deacetylases (HDAC3) and microRNAs (miR-155 and miR125b) have also been shown to play a role in the activation of macrophages to the pro-inflammatory phenotype (Perrot et al., 2023).

On the other end of the polarisation spectrum is the anti-inflammatory phenotype. Macrophages are polarised to an anti-inflammatory phenotype through stimulation with Th2 secreted cytokines IL-4 and IL-13 (Rőszer, 2015). Signalling pathways responsible for anti-inflammatory activation include STAT3, STAT6, PPARδ and PPARγ (Porta et al., 2015). The most important of the signalling pathways is STAT6, which has been shown to result in the activation and transcription of profibrotic genes (Liao et al., 2011). Anti-inflammatory macrophages act as anti-inflammatory mediators; thus, the context of this change in phenotype occurs during the resolution of inflammation and wound healing following an immune response (Laskin et al., 2011). The induction of such signalling cascades results in the upregulation of anti-inflammatory signalling molecules IL-1-R type II, IL-1Ra, IL-10, CCL18, and TGFβ (Arango Duque & Descoteaux, 2014). Additionally, these macrophages express scavenger receptors CD206 and CD163 as well as proteins FIZZ1, arginase-1, chitinase-3-like-1 and -2 (Perrot et al., 2023). Epigenetic factors that mediate anti-inflammatory polarisation include H3k27 demethylase Jumonji domain-containing protein-3 (Jmjd3) induced by IL-4 and miRNAs miR-223, -124, and -125a-5p and Let-c (Perrot et al., 2023).

1.6 Macrophages Drive Fibrosis Progression

The macrophage population within the lung is heterogeneous; thus, dissecting the exact mechanism of how macrophages contribute to lung fibrosis has been a topic of intense interest. Macrophages drive fibrosis and are integral to disease progression in the lung through production of signalling factors such as TGFβ (Arizmendi et al., 2014; S. Joshi et al., 2017). Pro-inflammatory macrophages are the first to respond after recruitment to the site of insult or injury in the lungs, where they combat pathogens and phagocytose debris while organizing an

appropriate inflammatory response (Younesi et al., 2024). Upon resolution, the microenvironment changes to promote healing and wound repair. At this point, macrophages shift toward an anti-inflammatory phenotype. Anti-inflammatory macrophages help reduce the wound bed by removing excess ECM, and in physiological repair, macrophages and myofibroblasts are eventually cleared by apoptosis, restoring normal tissue structure and enabling scarless healing. In fibrotic repair, however, contractile myofibroblasts and anti-inflammatory macrophages persist, continuing to drive ECM deposition and stiffening, which leads to excessive scarring (Ortiz-Zapater et al., 2022; Younesi et al., 2024). More specifically, macrophage-secreted TGFβ interacts directly with fibroblasts, causing their differentiation into myofibroblasts, which are a major source of collagen. Unfortunately, the interaction of macrophages with myofibroblasts is not limited to TGFβ secretion. Additionally, macrophages secrete insulin-like growth factor-1 (IGF-1), which prevents myofibroblast apoptosis and ultimately leads to an increase in collagen, which is produced by these cells (Perrot et al., 2023; T. Wynn & Barron, 2010). Growth factors such as platelet-derived growth factor (PDGF), vascular endothelial growth factor (VEGF), and fibroblast growth factor (FGF) are secreted by macrophages, interacting with fibroblasts and myofibroblasts through paracrine signalling to drive the fibrotic process (Li et al., 2021). Within the fibrotic lung, macrophages also play an important role in the structure of the ECM. Under homeostatic conditions, there is a constant cycle of ECM deposition and degradation. Profibrotic macrophages skew this cycle into one that favours deposition over degradation through the release of various matrix metalloproteinases (MMPs) and tissue inhibitors of MMPs (TIMPs) (Dancer et al., 2011; Perrot et al., 2023).

1.7 Altering Macrophage Phenotype by Employing Modified β-glucan and RP-182 Derived Nanoparticles

Several different therapeutic strategies that selectively target macrophages for numerous diseases are currently under investigation (Isshiki et al., 2023). One of these strategies is the repolarization of macrophages away from the profibrotic phenotype (Hu et al., 2021). Previous literature has shown the ability of β-glucan and a peptide called RP-182 to induce repolarization of anti-inflammatory profibrotic macrophages to a pro-inflammatory phenotype (Jaynes et al., 2020; Liu et al., 2015). β-glucans are an abundant natural product derived from the inner cell wall of fungi such as *Saccharomyces cerevisiae*. Immunomodulating β-glucans consist of a (1,3)-β-linked backbone with small numbers of (1,6)-β-linked side chains and are large as well as insoluble (Stier et al., 2014). Their large and insoluble properties lead to inconsistent bioavailability and poor diffusion into deep lung tissues, making it difficult to apply them for therapeutic purposes. Collaborators in McMaster's Department of Engineering have managed to formulate various soluble β-glucans with decreased size. These formulations include Polyelectrolyte Complex (PEC) and Self-Assembled (SA) β-glucan derivatives.

The second of the two compounds of interest is RP-182, a synthetically derived immunomodulator originally studied as a potential cancer therapeutic. Recently, a previous paper has shown RP-182 has the ability to induce a population shift in anti-inflammatory macrophages towards pro-inflammatory function and phenotype in a CD206-dependent manner *in vitro*. The group showed a rapid induction of CD86, a pro-inflammatory marker, in addition to increased cytokine production when profiling pro-inflammatory cytokines (Jaynes et al., 2020). Similar to the β-glucans, our collaborators in McMaster's Department of Engineering have produced RP-

182 nanoparticles that range in size from 500-100 nm through terminal linking of the RP-182 base peptide to polystyrene (PS) particles.

1.8 The Therapeutic potential of β-Glucan and RP-182 derived nanoparticles

β-glucan is a pattern recognition molecule that has been shown to trigger production of proinflammatory programming in macrophages (Liu et al., 2015). Dectin-1 is a non-classical C-type Lectin receptor that has been found to be highly expressed in pulmonary fibrosis and specifically on anti-inflammatory macrophages (Patel, 2018; Willment et al., 2003). Upon binding of β-glucan to Dectin-1, two pathways are initiated. These pathways are the Syk-dependent or independent pathways. Syk is a tyrosine kinase that also acts as an adaptor protein to phosphorylate downstream targets (Kulathu et al., 2009). The Syk-dependent pathway activates IRF5, NF-κβ, ERK, and PI3K, signalling to elicit the expression of various cytokines such as IL-1β, TNF-α, IL-8, IL-10, IL-12, and IL-2 along with phagocytosis and respiratory burst through ROS (Mata-Martínez et al., 2022). In addition, β-glucan has been shown to induce an innate immune memory response through Dectin-1/Raf-1/mTOR axis as well as a shift in metabolic pathways, inducing NADPH, a cofactor required for epigenetic enzymes (Cheng et al., 2024; Mata-Martínez et al., 2022).

In addition to β-glucan, RP-182 has been shown to be target specific, acting on the mannose receptor CD206. The surface receptor CD206, similar to Dectin-1, is a C-type lectin receptor that functions primarily to maintain immune homeostasis, scavenging for unwanted high-mannose *N*-linked glycoproteins as well as clearing pituitary hormones in circulation (Azad et al., 2014). Interest in CD206 comes from the fact that it is upregulated in both cancer as well as fibrosis and is commonly used as a primary biomarker for disease-associated macrophages

(Haque et al., 2019; Pommerolle et al., 2024). As mentioned, a previous group has shown the peptide RP-182 as an inducer of TNF, IL-1β, and IL-12, as well as upregulating CD86 when treating anti-inflammatory BMDMs and PBMCs *in vitro*. It does this through the binding and activation of CD206, inducing a conformational bend in the CRD4 and CRD5 domains of the receptor (Jaynes et al., 2020).

β-glucan nanoparticles, as well as the discovery of RP-182 as potential immunomodulating molecules, open a new avenue for the treatment of macrophage-associated diseases. By targeting disease-associated macrophage markers Dectin-1 and CD206, these nanoparticles may be able to directly alter macrophage phenotype and function in diseases such as pulmonary fibrosis. Furthermore, polyelectrolyte complexes (PECs), self-assembled (SA) and RP-182 materials have the potential to carry additional therapeutics directly to the fibrotic niche via transport by macrophages. Therefore, the employment of these nanoparticles opens a potential delivery system that can selectively target fibrotic areas of the lung, preventing off-target effects of therapeutics such as Nintedanib or Pirfenidone.

1.9 Hypothesis

We hypothesize that β-glucan and RP-182 derived nanoparticles will be preferentially taken up by pro-fibrotic macrophages, increasing pro-inflammatory surface marker expression, resulting in a change in macrophage phenotype.

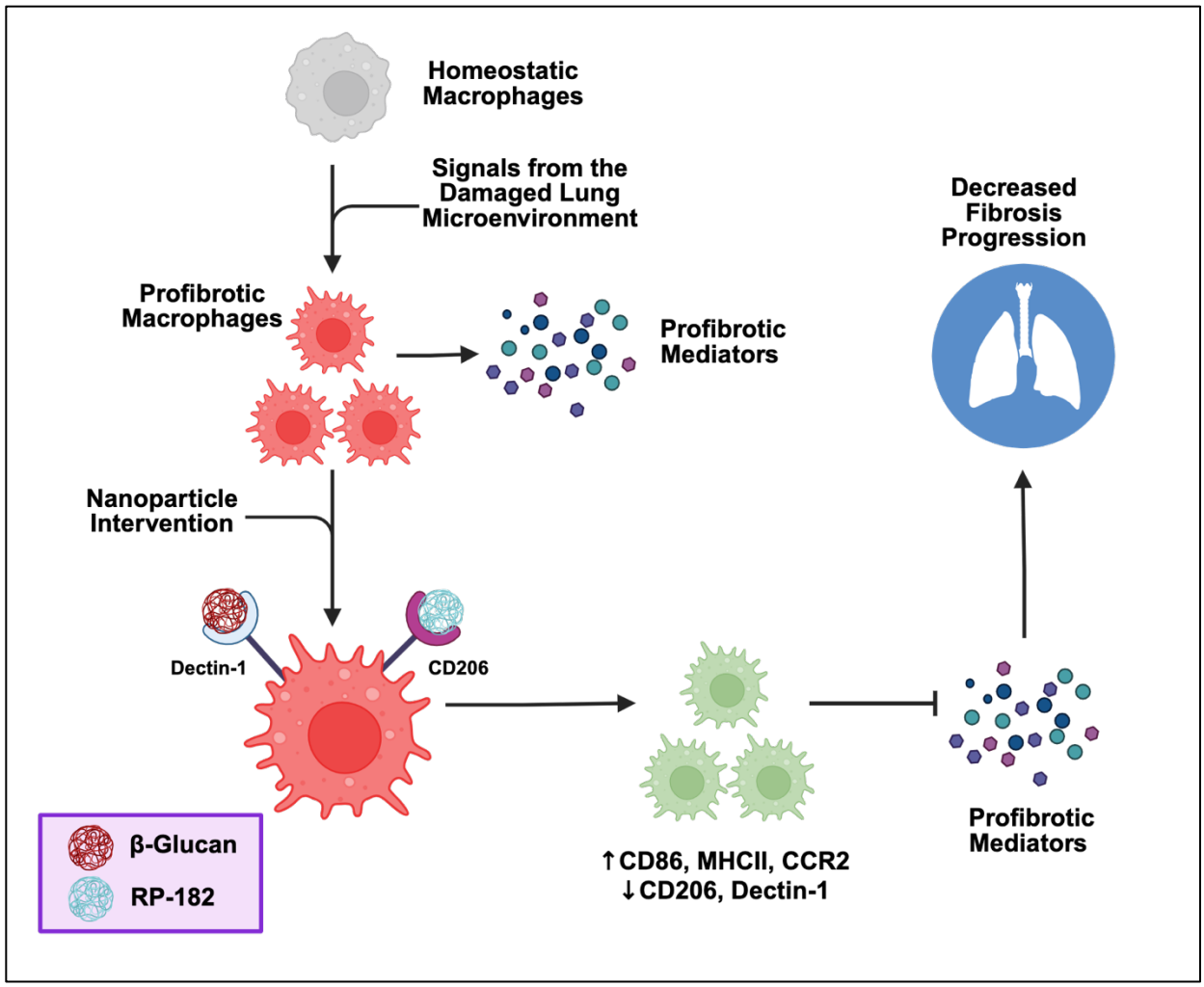

Figure 1.1 Graphical hypothesis of macrophage-mediated fibrosis and β-glucan as well as RP-182 nanoparticle intervention. Macrophages transition toward a pro-fibrotic phenotype, upregulating receptors such as Dectin-1 and CD206. Our study aims to exploit these receptors by using nanoparticle formulations incorporating β-glucan and RP-182 to modulate macrophage phenotype to limit fibrotic progression.

Chapter 2: Materials and Methods

2.1 Isolation of Bone Marrow-Derived Macrophages

Bone marrow was isolated from the spines of young (<6 mo) wild type (WT) C57BL/6J mice. Hematopoietic progenitors were cultured for 7 days with RPMI supplemented with 15% L929 Conditioned Media (LCM), 10% fetal bovine serum, 2 mM L-Glutamine, 100 U/mL penicillin (R10+15% LCM) to induce differentiation into macrophages per the Bowdish lab protocol (Shayhidin et al., n.d.). After 7 days, differentiated macrophages were lifted and stored for future use.

2.2 Macrophage Polarization & Stimulation

Macrophages isolated from WT C57BL/6J mice were thawed and cultured with R10 media (15% LCM) overnight in petri dishes. The following day, macrophages were stimulated with a combination of carrier-free recombinant mouse IL-4 (20 ng/mL), IL-13 (50 ng/mL), and IL-6 (5 ng/mL) to achieve the anti-inflammatory phenotype. To achieve a pro-inflammatory macrophage phenotype, carrier-free recombinant mouse IFNγ (50 ng/mL) and lipopolysaccharide (10 ng/mL) were used. Cells were cultured for 48 hours with IL4/13/6 or 24 hours with LPS+IFNγ cytokine mixes in R10 media (15% LCM) to achieve either pro- or anti-inflammatory BMDM phenotype. Cytokines and associated catalogue numbers can be found in Table 2.1.

Table 2.1 Cytokines used for *in vitro* BMDM and PCLS stimulation.

CYTOKINE	CONCENTRATION	SOURCE
IL-4	20 ng/mL	Biolegend (574302)
Il-13	50 ng/mL	Biolegend (575902)
IL-6	5 ng/mL	Biolegend (575702)
LPS	10 ng/mL	Thermofisher (00-4976-93)
IFNγ	50 ng/mL	Biolegend (575302)

2.3 Flow Cytometry

Following treatment or stimulation of BMDMs, cells were lifted using Accutase cell detachment media (Thermofisher Cat: 00-4555-56) and pelleted at 1500 rpm in 5 mL tubes. Cells were then resuspended in 200 µL of 1x Phosphate Buffered Solution (PBS). To determine potential depletion of BMDMs in response to nanoparticle treatment, a live/dead stain was incorporated (BD Biosciences Cat: 565694), and cells were stained for 12 minutes at room temperature. This was followed by decanting of the supernatant and a subsequent wash with 1x PBS, repeated three times. After the third wash and centrifugation, cells were resuspended and incubated in Fc block (BioLegend Cat: 101319) at a volume of 50 µL for a dilution of 1:10 for 15 minutes at room temperature. To measure surface receptor expression, BMDMs were stained using monoclonal antibodies with conjugated fluorophores (Table 2.2) in a total volume of 50 µL for 30 minutes at room temperature. Cells were washed with 1x PBS, centrifuged, and resuspended in 200 µL 1x Fix-Lyse buffer (ThermoFisher Scientific, cat: 00-5333-52). Plates

were incubated at room temperature for 8 minutes. Following fixation, cells were resuspended in 200 µL 1x PBS once and then spun down again and resuspended in 240 µL FACS wash (5 g/L Bovine Serum Albumin, Sigma-Aldrich Cat: A2153; 5 mM EDTA, BioShop Canada, Cat: EDT001.500) and kept at 4˚C before filtering for flow cytometry analysis. Flow cytometry was conducted using a Beckman Coulter CytoFLEX Flow Cytometer. Analysis was performed using FlowJo v10 software. An illustration depicting this gating strategy can be seen in Supplementary Figure 1.

Table 2.2 Antibodies used in our Phenotyping Assay to assess changes in BMDM surface receptor expression.

MARKER	FLUOROPHORE	VOLUME	CONCENTRATION	ISOTYPE	SOURCE
MHCII	APC-ef780	0.5	1:100	Rat IgG2a, K	Invitrogen (47-5321-82)
CCR2	BV421	0.625	1:80	Rat IgG2b, K	Biolegend (150605)
CD86	RB705	0.0325	1:1500	Rat IgG2a, K	BD Horizon (570689)
DECTIN-1	PE	0.625	1:80	Mouse IgG1, K	BD Pharmingen (568714)
CD206	BV785	0.167	1:300	IgG2a, K	Biolegend (141729)
F4/80	APC	0.2	1:250	N/A	Invitrogen (17-4801-82)

2.4 Precision Cut Lung Slices

Animals were anesthetized with isoflurane and exsanguinated by severing the inferior vena cava. After sacrifice, the lungs were perfused by injecting 5 mL of warm PBS into the right ventricle of the heart to flush out residual blood. The trachea was cannulated, and 1.3 mL of 40 °C 1.5% low-melting-point agarose (Invitrogen) dissolved in PBS was slowly infiltrated into the lungs via the cannula, followed by a 0.2 mL bolus of air to ensure agarose reached the lower airways. After the lungs were inflated, the perfused mice were transferred onto ice and left to cool for 5 min to ensure complete gelling of agarose prior to excision of lungs. Lungs were then carefully excised, and lobes were separated. Each lobe was then affixed to a specimen holder, externally embedded in 2% agarose, and individually sliced (300 μm thickness) in PBS using a Compresstome VF-510-0Z vibrating microtome (Precisionary Instruments; speed setting: 1.5, oscillation setting: 8). PCLS cores (4 mm diameter) were obtained from full slices using a tissue puncher. After slicing, PCLS were cultivated in DMEM culture medium supplemented with 10% fetal bovine serum, 2 mM L-Glutamine, 100 U/mL penicillin, and 2.5 μg/mL amphotericin B at 5% CO_2. The media was changed 3 times, and PCLS were left in the incubator overnight to acclimate prior to treatment. At the time of treatment, PCLS were moved to 12-well plates and treated with a recombinant IL-4 (20 ng/mL), IL-6 (5 ng/mL), and IL-13 (50 ng/mL) or media only. Stimulation was done over 48 hours. Slices were then incubated for an additional 48 hours with media only.

2.5 Uptake Assay

Following incubation, specific wells were treated with heat-inactivated goat serum used as an IgG control or media only for 1 hour. This was subsequently followed by treatment with a polyclonal goat anti-Dectin-1 antibody or media as a vehicle control, and incubation for 1 hour. The cells were subsequently washed, and this was followed by a 90-minute incubation period with Fluoresbrite YG PS beads (Polyscience Cat: 17150), PS conjugated with RP-182, or media only at 37°C and duplicate plates at 4°C. Following incubation, cells were washed 3x with PBS and imaged using an EVOS. Live Cell Imager (12-well plates) or read at a wavelength of 519 using an Agilent BioTek Synergy H1 Microplate Reader (96-well plates).

2.6 Precision Cut Lung Slice RNA Isolation, cDNA Synthesis, and 2-Step RT-qPCR

RNA Isolation

In short, 6 slices per condition were washed 3x with 1x PBS and placed in 400 µL RNAsave. The slices were then left at 4°C for 24 hours before being frozen -80 °C until extraction. To isolate RNA, slices were thawed and placed in 800 µL TRIzol reagent (Invitrogen, cat: 15596026) in 2 mL homogenization tubes with 5 2.8 mm (VWR, cat: 10158-612). Homogenization tubes were loaded into the MP Fast Prep-24 benchtop homogenizer at a speed of 6 m/s for 60 seconds. Following homogenization, the lysates were moved into new 2 mL Eppendorf tubes and centrifuged at 16,000 xg and 4°C for 10 minutes. The supernatant was then transferred to a new 2 mL Eppendorf and left at room temperature for 5 minutes to allow for nucleoprotein complex dissociation to occur. This was followed by the addition of anhydrous ethanol at a 1:1 ratio of ethanol to TRIzol (800 µL). RNA was then isolated using the Zymo Direct-zol RNA microprep kit (Avantor Sciences, cat: 76020-642). After following the kit

protocols, RNA was eluted in a volume of 12 ng/ µL. The concentration of RNA was measured and standardized to 100 ng/µL (±25 ng/µL) using a nanodrop spectrophotometer. Samples were stored at -80 °C until further use.

cDNA synthesis and 2-Step RT-qPCR

cDNA was synthesized from extracted PCLS RNA for quantitative reverse transcription polymerase chain reaction (RT-qPCR). 1 µL of 10 mM dNTPs and 1 µL of 10 µM random pentadecamers were added to 8 µL of standardized RNA in a PCR tube. The mix was incubated at 65°C for 5 minutes and then placed on ice for 1 minute. 9 µL of the 2x reaction mix (4 µL of 5x FS buffer, 2 µL of 0.1 M DTT, 2 µL of 50 mM MgCl2, 1 µL of 40 U/µL RiboLock RNase Inhibitor (ThermoFisher Scientific, cat: EO0382) was added, and the mixture was left to stand at room temperature for 2 minutes. 1 µL of SuperScript™ II Reverse Transcriptase (ThermoFisher Scientific, cat: 18064014) was added to each tube. A negative control tube where samples underwent all the same steps but with the addition of 1 µL of nuclease-free water instead of the enzyme was also set up. In a thermocycler, samples and controls were incubated at 25 °C for 10 minutes, 42 °C for 50 minutes, and finally 70 °C for 15 minutes to terminate the reaction. Samples were stored at -20 °C until 2-step RT-qPCR.

For RT-qPCR, cDNA was diluted 10-fold with nuclease-free water. A 1x qPCR master mix was created for each sample according to the following recipe: 5 µL of 2x GoTaq qPCR Master Mix (Promega, cat: A6001), 1 µL of Forward Primer, 1 µL of Rev Primer (Integrated DNA Technologies, custom DNA oligo), 0.1 µL of CXR Dye(Promega, cat: A6001), and 0.4 µL of Nuclease-free water. A new master mix was created for each primer pair.

7.5 µL of each target-specific 1x qPCR master mix was added to 2.5 µL of 1:10 cDNA in a 96-well PCR reaction plate. Duplicate wells were set up for each sample, as well as a non-template

control, which received the master mix and 2.5 µL of nuclease-free water instead of cDNA template, and an inter-run control (IRC) containing a mixture of cDNA from all samples. The plate was centrifuged at 1,200 g at 22 °C for 1 minute and loaded into the qPCR thermocycler with the following thermocycler cycling conditions (Table 2.3).

2.7 Arginase Activity Assay

The arginase assay was performed on $8x10^4$ cells in 96-well plates as outlined previously (Ayaub et al., 2017; Vierhout et al., 2024). Following treatment, cells were lysed in 25 µL of 0.1% Triton X-100 supplemented with protease inhibitors and phosphatase inhibitors. A 1:1 dilution with 25 mM of Tris-HCl (pH 7.5) was later performed. 25 µL of this mixture was transferred to PCR tubes, with the addition of 2.5 µL of 10 mM manganese chloride. The tubes were then placed in a thermal cycler programmed to heat at 56°C for 10 minutes. After incubation, 25 µL of 0.5 M L-arginine was added to the mixture and tubes were then incubated at 37°C for 30 minutes. An eight-point urea standard curve was then established (0.625 to 20 mM). 200 µL of acid solution (63.6% water, 9.1% concentrated sulphuric acid and 27.3% concentrated phosphoric acid), followed by 10 µL of 9% alpha-isonitrosopropiophenone, were added to both samples and the urea standards. The contents of each tube were mixed thoroughly and subsequently incubated at 95°C for 30 minutes, followed by 5 minutes of cooling at 20°C. 150 µL of each sample was removed and placed in a new, clear, flat-bottom, 96-well plate for absorbance reading at 550 nm using an Agilent BioTek Synergy H1 Microplate Reader.

2.8 Statistics

Results were expressed as the mean ± standard error of the mean (SEM). Comparisons of two groups were performed with an unpaired two-tailed *t*-test, while more than two groups were compared with ANOVA statistical analyses using GraphPad Prism 10. A p-value less than 0.05 was considered statistically significant

Table 2.3. Thermocycler cycling conditions for 2-step RT-qPCR.

	Temperature (°C)	Time (seconds)
Holding Stage	95	20
Cycling Stage (40x)	95	3
	60	30; read
Melting Curve Stage	95	15
	60	60
	Transition: +0.3	Read
	95	15; read

Table 2.4. Primer Sequences used in 2-Step RT-qPCR.

Target	Forward Primer	Reverse Primer
Nos2	5’ - CAGCTGGGCTGTACAAACCTT - 3’	5’ - CATTGGAAGTGAAGCGGTTCG-3’
Tnfa	5’- CAGGCGGTGCCTATGTCTC - 3’	5’ - CGATCACCCCGAAGTTCAGTAG - 3’
Chil3	5’- TTTGGACCTGCCCCGTTCAG - 3’	5’ - CTCCACAGATTCTTCCTCAAAAGC - 3’
Col1a1	5’- CGATGGATTCCCGTTCGAGT - 3’	5’ - CGATCTCGTTGGATCCCTGG - 3’
Fn1	5’- CCTCCCGTTCACCTACAACG - 3’	5’ - TCTGAACCAAAACCGCATGG - 3’
Acta2	5’- CGTGACTACTGCCGAGCGT - 3’	5’ - TAGGTGGTTTCGTGGATGCCC - 3’
Tgfb	5’- CTGATACGCCTGAGTGGCTG - 3’	5’ - TTTGGGGCTGATCCCGTTG - 3’
Ppia	5’- CTTCGAGCTGTTTGCAGACA - 3’	5’ - TGGCGTGTAAAGTCACCAC - 3’

Chapter 3: Model Validation and β-glucan nanoparticle treatment of BMDMs increases pro-inflammatory marker expression

3.1 In-vitro BMDM Model Validation

We first began by validating our 'pro-fibrotic' anti-inflammatory *in vitro* macrophage model to ensure we could detect changes in macrophage phenotype through increases in specific surface receptors. The surface receptors that were chosen included CD86, MHCII, CCR2, C-type lectin receptor Dectin-1, and the mannose receptor CD206. The co-stimulatory receptor CD86, antigen presentation receptor MHCII, and macrophage recruitment receptor CCR2 were chosen as pro-inflammatory markers due to their extensive use throughout the field. C-type lectin receptor Dectin-1 and the mannose receptor CD206 were chosen due to their use as anti-inflammatory macrophage markers within the literature (Perrot et al., 2023), in addition to the hypothetical interactions we expected to see regarding our nanoparticle formulations and their bioactive additives, β-glucan and RP-182, respectively.

BMDMs were stimulated *in vitro* with either LPS+IFNy for 24 hours, or IL4/13/6 for 48 hours, followed by the quantification of surface marker expression via flow cytometry. Values were then expressed as geometric mean fluorescent intensity relative to the media only control. LPS is an extremely potent pro-inflammatory stimulant that is recognized by CD14 and transferred to the TLR4-MD2 complex, leading to MyD88 and TRIF signalling cascades. This cascade ultimately leads to NFκβ and MAPK activation and pro-inflammatory cytokine production that is amplified by the addition of IFNγ (Groettrup et al., 2001; Reis et al., 2011; Vasudevan et al., 2022). Stimulation with IL-4 and IL-13 activates JAK–STAT6 signalling to induce an alternatively activated macrophage phenotype characterized by increased CD206 surface receptor expression. IL-6 enhances STAT3 activity and upregulates IL-4R expression, thereby amplifying responsiveness to IL-4/IL-13 and reinforcing anti-inflammatory polarization

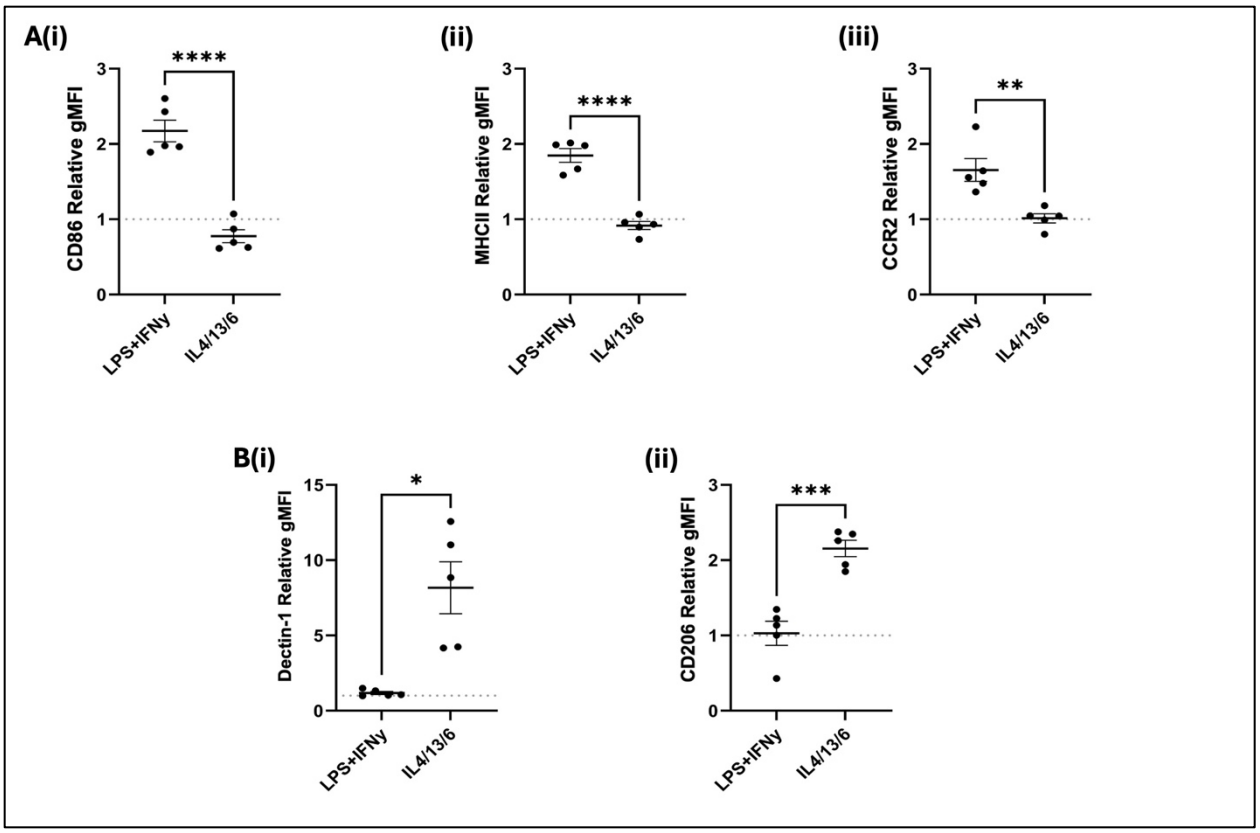

Figure 3.1 Distinct surface marker profiles confirm polarization model validity.

Pro-inflammatory (A) and anti-inflammatory (B) surface marker expression shown as relative geometric mean fluorescent intensity (gMFI) determined by normalizing stimulated condition samples to their respective unstimulated controls. Statistical significance was analyzed by unpaired two-tailed Student's t-test (p=0.05). n=6 biological replicates, 2 samples across three independent experiments. Error bars represent mean ± SEM, *$p < 0.05$, **p<0.01.

(Gupta et al., 2018; Scott et al., 2023). As expected, LPS+IFNy treated BMDMs exhibited significant increases in surface marker expression of all pro-inflammatory markers (i.e., CD86, MHCII, CCR2) with no changes in expression of those markers on cells treated with the IL4/13/6 anti-inflammatory cytokine mix (Fig. 3.1A). Inversely, IL4/13/6 stimulation of BMDM resulted in significant upregulation of surface marker expression of the anti-inflammatory markers Dectin-1 and CD206, with no increases in cell surface expression of those markers after LPS+IFNy stimulation (Fig. 3.1B). Therefore, our *in vitro* BMDM model worked as expected.

To further support our model, we wanted to examine whether the changes in BMDM phenotypes induced by IL4/13/6 stimulation might also result in a functional shift. Colorimetric arginase activity assays were used to answer this question. The enzyme arginase diverts L-arginine away from iNOS to promote tissue repair and dampen inflammation. The assay itself quantifies the ability of arginase within cell lysate to catabolize a known amount of L-arginine into urea, a downstream product of the L-arginine degradation pathway. By using the arginase assay, we aimed to compare the functional profiles of IL4/13/6 stimulated BMDMs with both unstimulated (media only) and LPS+IFNy treated BMDMs. No change in urea concentration was seen after BMDM treatment with LPS+IFNy, as values were consistent with the media only control (Fig. 3.2). Results showed significant increases in millimolar urea concentrations detected compared to the media only control.

An important aspect when assessing the efficacy of nanoparticle materials as macrophage-mediated therapeutics for fibrosis was to ensure that we could capture a pro-inflammatory shift in surface marker expression induced by these materials. Following the validation of our model, we then considered whether BMDMs pre-treated with IL4/13/6 for 48 hours to achieve an anti-inflammatory phenotype could be pushed to elicit a pro-inflammatory

phenotype when subsequently subjected to a pro-inflammatory stimulus such as LPS and IFNγ. This is important as our nanoparticle formulations were expected to induce a pro-inflammatory response to shift macrophage phenotype away from its anti-inflammatory, pro-fibrotic phenotype.

Following the initial 48-hour pre-stimulation treatment with IL4/13/6 cytokines, cells were either left untreated (i.e., media only after the initial stimulation) or stimulated with LPS+IFNγ for 24 hours before quantification of surface marker expression profiles. As expected, BMDM surface expression of CD86, MHCII, and CCR2 all increased significantly after combined IL4/6/13 and LPS+IFNγ treatment when compared to BMDMs only pre-stimulated with IL4/13/6 only condition (Fig. 3.3A). Conversely, Dectin-1 relative mean fluorescence intensity decreased approximately two-fold after stimulation with the potent pro-inflammatory stimulants LPS and IFNγ, indicating decreased receptor expression of one of the two anti-inflammatory markers (Fig. 3.3B). CD206, the second of the two anti-inflammatory markers, unexpectedly showed no significant increase or decrease in receptor expression, contrary to an expected increase after pro-inflammatory stimulation (Fig. 3.3B (ii)).

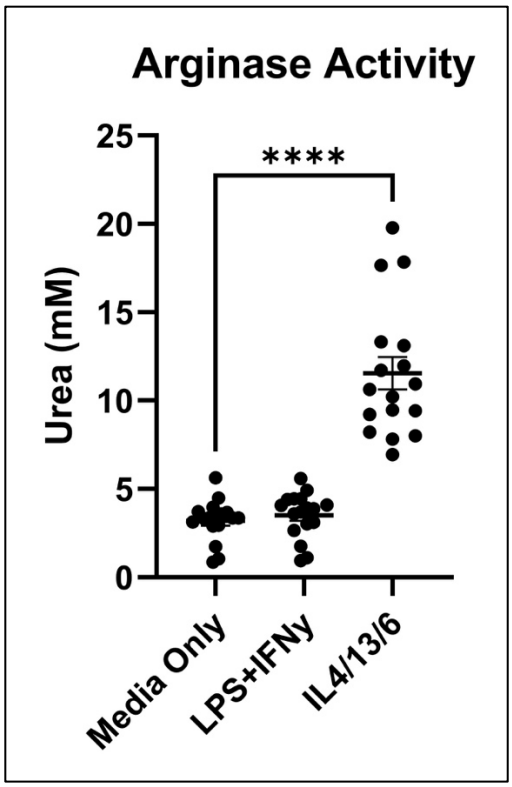

Figure 3.2 IL4/13/6 stimulation increases arginase activity in BMDMs. Arginase activity was quantified in BMDMs following 48-hour stimulation with IL4/13/6 using a colorimetric urea production assay, confirming enhanced alternative activation relative to LPS+IFNγ and untreated controls**.** Statistical significance was analyzed by one-way ANOVA with Tukey's multiple comparisons of the mean of conditions to the mean of the IL4/13/6 control group (p=0.05), n=17 biological replicates. Error bars represent mean ± SEM, ****p<0.0001.

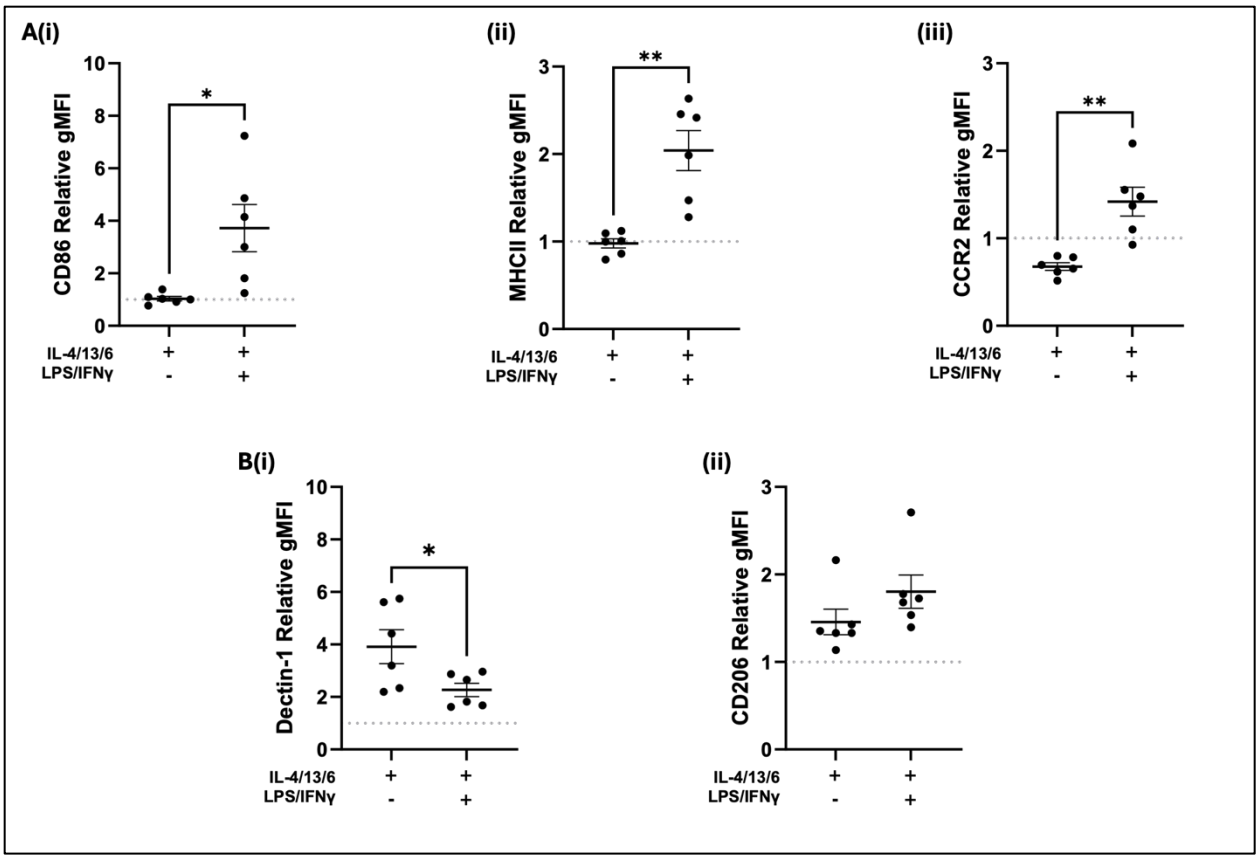

Figure 3.3. Pro-inflammatory stimulation overrides most surface marker changes induced by IL4/13/6 pre-treatment. BMDMs were pretreated with IL4/-13/-6 followed by LPS+IFNγ stimulation or media only to assess phenotypic plasticity. Pro-inflammatory (A) and anti-inflammatory (B) surface marker expression shown as relative geometric mean fluorescent intensity (gMFI) determined by normalizing conditions to an unstimulated, non-pretreated control. Statistical significance was analyzed by unpaired student's t-test (p=0.05). n=6 biological replicates, 2 samples across three independent experiments. Error bars represent mean ± SEM, *$p < 0.05$, **p<0.01.

3.2 Phenotyping of Anti-Inflammatory Bone Marrow-Derived Macrophages Following Treatment with β-Glucan Nanoparticle Materials

A large component of this project focused on assessing macrophage phenotypic and functional responses to β-glucan derived materials, provided by the Hoare Lab from McMaster's Department of Chemical Engineering. Two different nanoparticle platforms were used for these β-glucan derived materials. The first platform was the Polyelectrolyte Complex (PEC), which consisted of polyanionic glucan sulphate and polycationic dextran glycidyl trimethylammonium chloride (GTAC) that self-assembles via electrostatic forces in solution to form the complex. The PECs were loaded with Doxorubicin (DOX), a well-studied chemotherapeutic (Thi et al., 2021). The second of the two platforms is the Glucan Sulphate Self-Assembled nanoparticle (SA). The SAs are similar to PECs but replace the Dextran GTAC with Poly(oligo(lactic acid) methacrylate), or POLAMA, which is engrafted onto the glucan sulphate backbone. These complexes then self-assemble in solution via hydrophobic forces driven by the POLAMA branches to create a POLAMA-concentrated core with a glucan shell.

As we had validated our model and its ability to detect changes in surface marker expression after an initial IL4/13/6 stimulation, the next step was to begin assessing the macrophage-modifying activities of the DOX-PEC and SA nanoparticle materials. We first assessed if our materials were capable of inducing a pro-inflammatory response characteristic of Dectin-1 activation, similar to what was seen in our repolarization experiment (Fig. 3.3). Thus, using our *in-vitro* model, we treated anti-inflammatory BMDMs

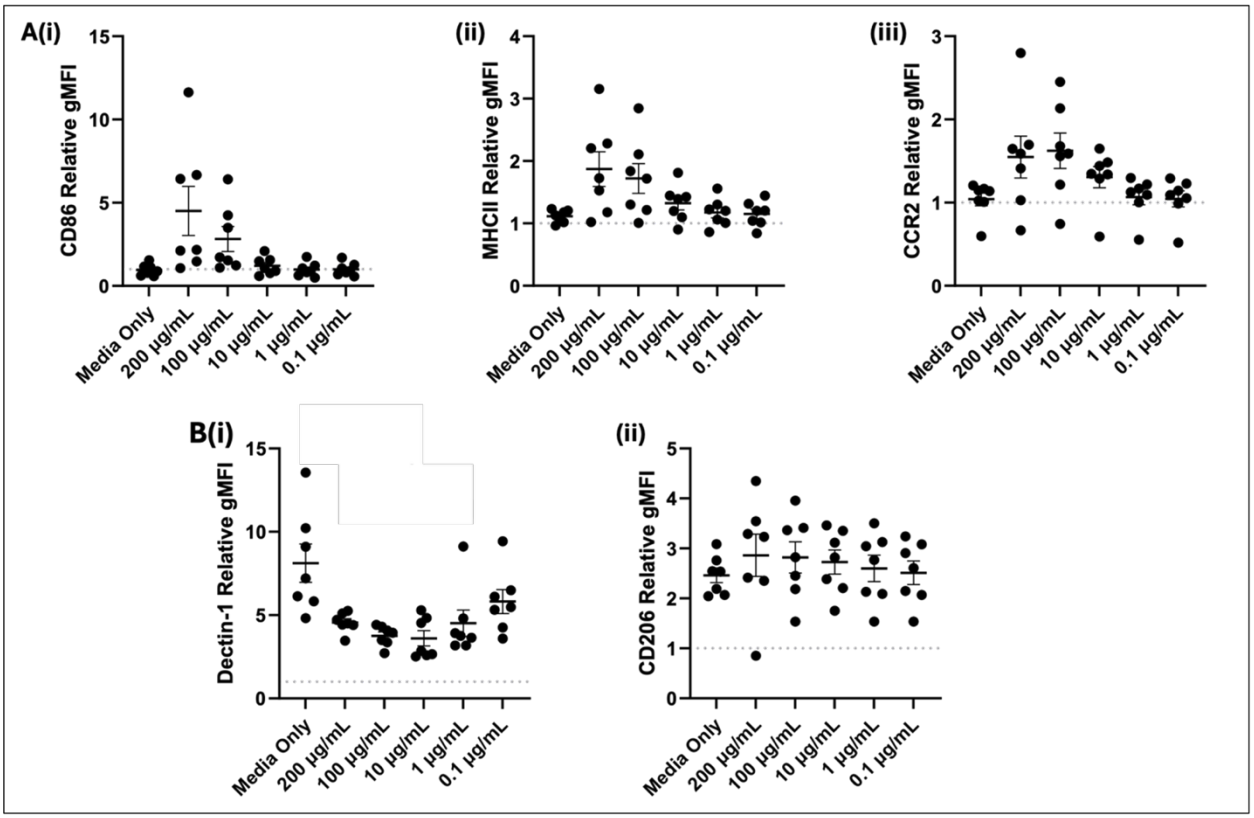

Figure 3.4. DOX-PEC β-glucans alter macrophage phenotype towards pro-inflammatory.

Pro-inflammatory (A) and anti-inflammatory (B) surface marker expression shown as relative geometric mean fluorescent intensity (gMFI) determined by normalizing conditions to an unstimulated, non-pretreated control. All tested concentrations (200 µg/ml down to 1 µg/ml) produced significantly elevated responses compared to the media-only negative control ($p < 0.01$). Statistical significance was analyzed by one-way ANOVA with Tukey's multiple comparisons of the mean of conditions to the mean of the IL4/13/6 control group ($p=0.05$), n=7 biological replicates across three individual experiments. Error bars represent mean ± SEM.

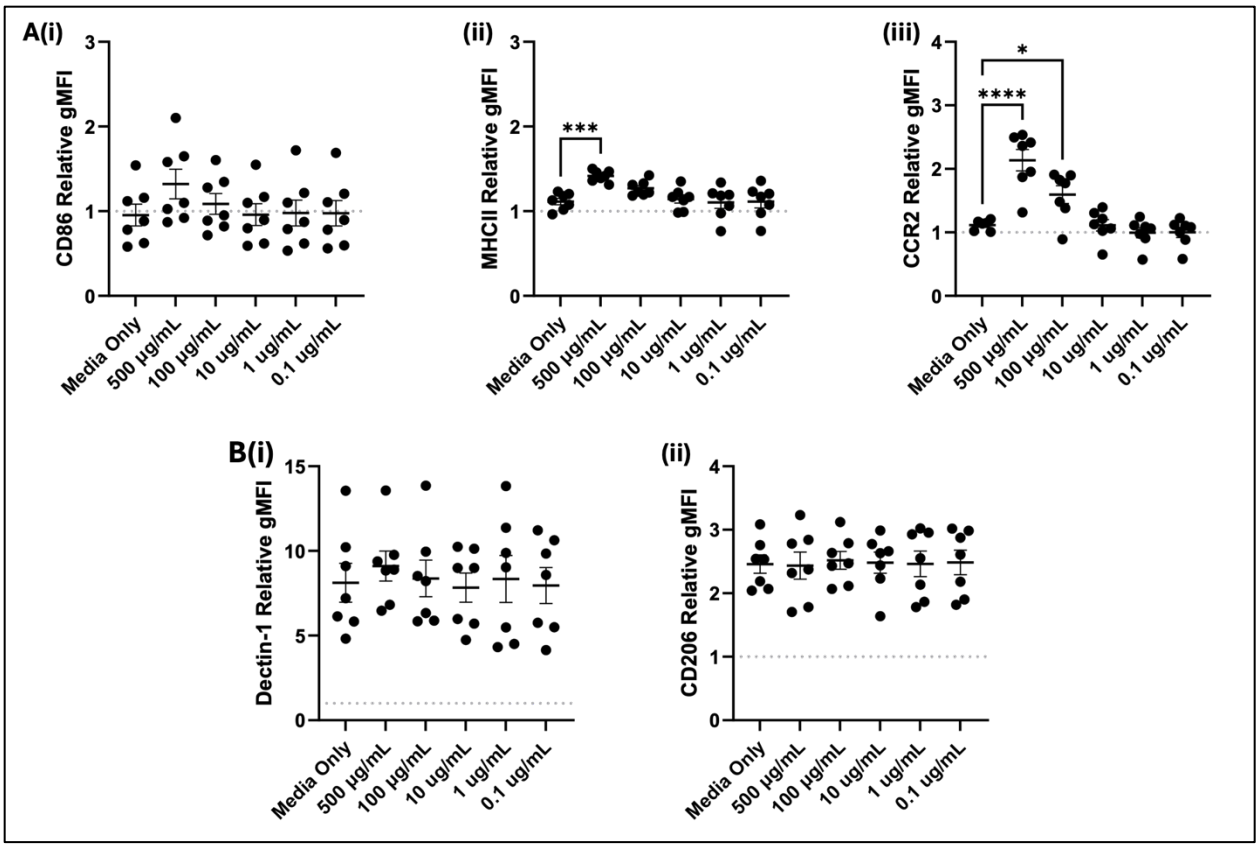

Figure 3.5 SA β-glucans induce an increase in pro-inflammatory surface marker expression. Pro-inflammatory (A) and anti-inflammatory (B) surface marker expression shown as relative geometric mean fluorescent intensity (gMFI) determined by normalizing conditions to an unstimulated, non-pretreated control. Statistical significance was analyzed by one-way ANOVA with Tukey's multiple comparisons of the mean of conditions to the mean of the IL4/13/6 control group (p=0.05), n=6 biological replicates across three individual experiments. Error bars represent mean ± SEM, Error bars represent mean ± SEM, *p<0.05, ***p<0.001, ****p<0.0001.

with decreasing concentrations of PECs and SA materials for 24 hours and assessed surface marker expression via flow cytometry. SA β-glucan nanoparticles showed a non-significant increase in CD86, most likely due to high variability in the data. However, SA β-glucans elicited a statistically significant upregulation of both MHCII and CCR2 at treatment concentrations of 500 μg/mL (Fig. 3.5A). Additionally, SA β-glucan nanoparticles had no effect on Dectin-1 and CD206 (Fig. 3.5B). In conjunction with the β-glucan materials, DOX PECs were assessed. All three pro-inflammatory markers increased, represented by an approximate 8-fold increase in CD86, a 2-fold increase in MHCII, and a 1.5-fold increase in CCR2, although not mounting any significance across all three markers (Fig. 3.4A). DOX PECs also induced a significant decrease in Dectin-1 (4-fold) at concentrations greater than 1 μg/mL but showed no change in CD206 expression (Fig. 3.4B).

3.3 PCLS Validation and Treatment with SA Nanoparticles

The use of monocultures such as BMDMs only provides insight into the effects of the nanomaterials on a single cell type. It is important when exploring the potential of any therapeutic to take a more holistic approach, especially for a disease such as fibrosis, where its progression is influenced by multiple cell types and a complicated cytokine milieu. The development of effective therapies for pulmonary fibrosis requires models that accurately reflect the complex cellular and structural environment of the fibrotic lung. Precision-cut lung slices provide a highly relevant *ex vivo* platform for drug evaluation, as they preserve the three-dimensional architecture of the lung, including the spatial organization of epithelial cells, fibroblasts, immune cells, and the extracellular matrix (Koziol-White et al., 2024).

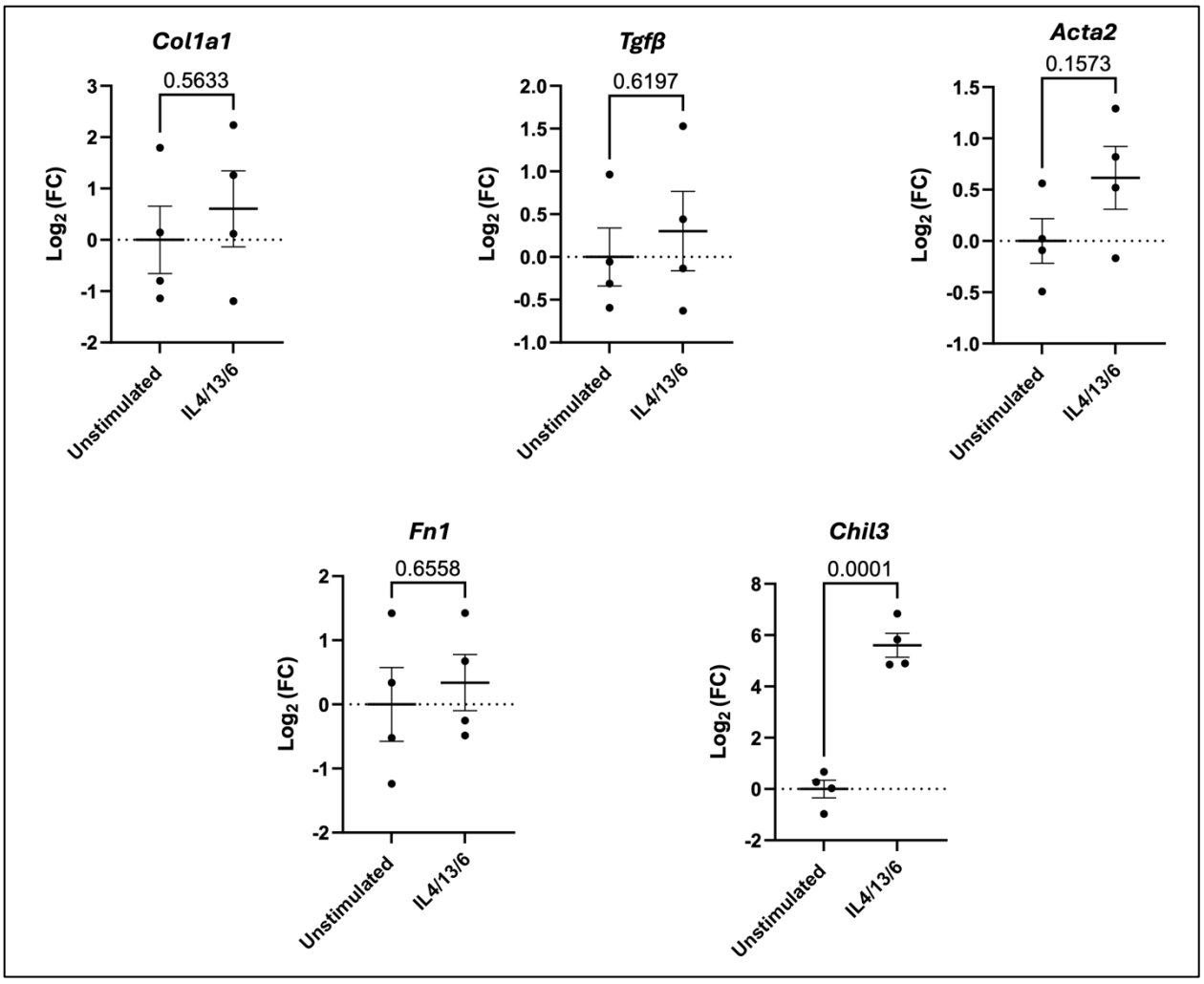

Figure 3.6 IL4/13/6 increases macrophage-specific markers but fails to elicit any significant change in ECM component gene expression. PCLS slices were left unstimulated or stimulated for 48 hours. Statistical significance was analyzed by unpaired student's t-test (p=0.05), n=4 biological replicates across three individual experiments. Error bars represent mean ± SEM.

To validate our PCLS model of fibrosis, 300 μm thick lung slices were stimulated with IL4/13/6. Slices were then processed, RNA was extracted, and RT-qPCR was performed. We examined the expression of gene targets specific to resident macrophages, myofibroblasts, as well as ECM components to assess our capacity to initiate the fibrotic process. Genes associated with myofibroblast activation and ECM remodelling (Table 3.1) had higher expression after IL4/13/6 treatment than the unstimulated control, but failed to reach statistical significance. Interestingly, macrophage activation marker *Chil3* was heavily upregulated in the stimulated condition and was highly significant (Fig. 3.6). Although we saw minimal increases in gene expression of ECM components or TGFβ, the increase in *Chil3* after IL4/13/6 stimulation suggested a successful shift in macrophage phenotype. A limitation of the PCLS model is its high demand for both resources and time, making it impractical to apply across all nanoparticle candidates. To maximize efficiency, we prioritized the more promising SA nanoparticle platform for further investigation. In this next phase, we also increased our gene candidates by including the pro-inflammatory genes *Tnf* and *Nos2*. We expected that monitoring expression of these markers would allow us to assess the platform's capacity to elicit a robust inflammatory response in lung tissue, providing insight into its potential as an immune-stimulating or immunomodulatory therapeutic.

Similar to the model validation experiment, 300-μm thick slices were stimulated with IL/4/13/6 for 48 hours, followed by a 48-hour nanoparticle treatment period. Six slices per condition were then processed, RNA was extracted, and gene expression was analyzed via RT-qPCR. As previously observed in Figure 3.6 above, *Chil3* increased significantly as a result of IL4/13/6 stimulation. Although there is a slight decrease in *Chil3* gene expression after SA

Table 3.1 Function of RT-qPCR genes of interest.

Gene	Function	Reference
Collagen type I alpha-1 chain *(Col1a1)*	• Primary structural protein of the ECM • Upregulated by myofibroblasts and anti-inflammatory macrophages	(Chen et al., 2021; Madsen et al., 2013)
Transforming Growth Factor β *(Tgfβ)*	• Potent inducer of mesenchymal gene expression, causing the transition of fibroblasts, epithelial cells, and endothelial cells into myofibroblasts • Highly expressed and secreted by macrophages, T-regulatory cells, and T helper 17 cells	(Desai et al., 2018; Meng et al., 2016)
α-smooth muscle actin *(Acta2)*	• Contributes to cell-generated mechanical tension that contributes to ECM remodelling • Highly upregulated by myofibroblasts	(Shinde et al., 2017; Wang et al., 2006)
Fibronectin *(Fn1)*	• Critical ECM component • Regulates adhesion, proliferation, migration, differentiation, and cytokine release • Primarily produced by myofibroblasts	(Bonadio et al., 2024)
Chitinase-like protein *(Chil3)*	• Member of chitinase-like proteins • Chitin-degrading enzyme that plays a protective role in innate immunity against chitin-containing pathogens including parasites, fungi, and arthropods • Highly expressed in anti-inflammatory macrophages	(Kang et al., 2022)
Tumour necrosis factor (*TNF*)	• Pro-Inflammatory cytokine that drives the immune cell activation and contributes to tissue inflammation • Indicator of pro-inflammatory macrophage activation	(Jang et al., 2021; Lu et al., 2018)
Inducible Nitric Oxide Synthase (*iNOS*)	• Catabolizes L-arginine into nitric oxide • Induced by pro-inflammatory cytokines and signalling molecules such as TNF • Upregulated in pro-inflammatory macrophages	(Anavi & Tirosh, 2020; Xue et al., 2018)

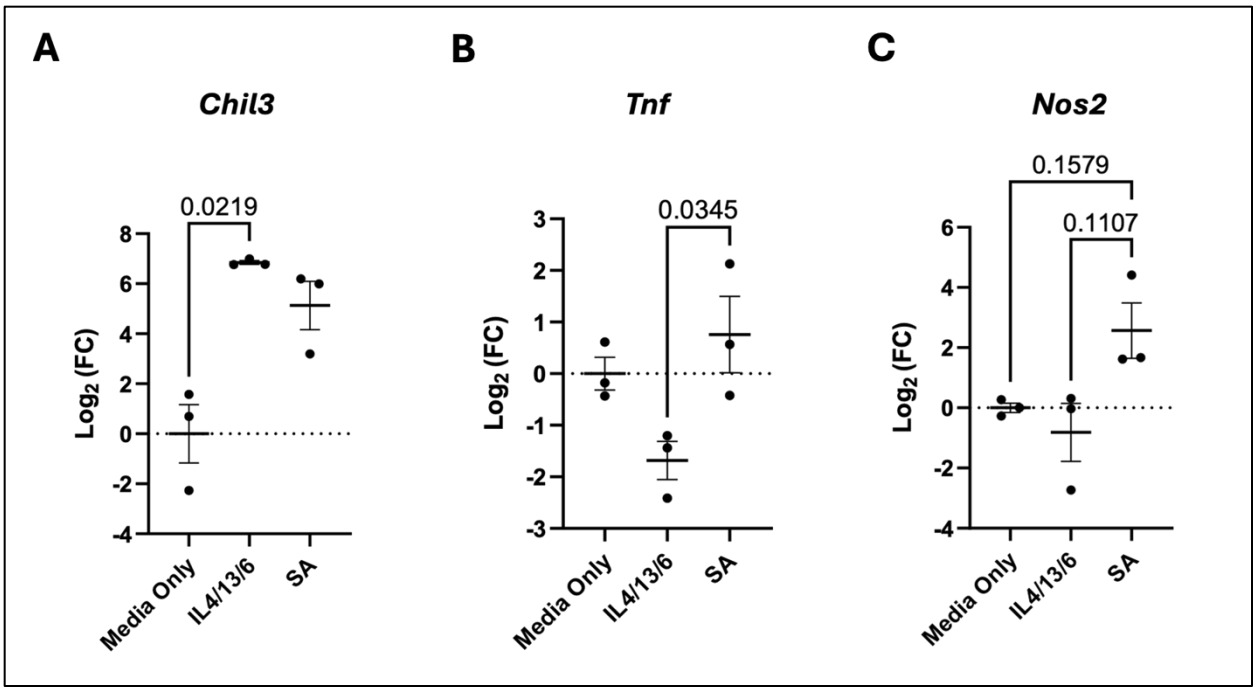

Figure 3.7 SA nanoparticle treatment increases expression of inflammatory activation markers in BMDMs. Statistical significance was analyzed by one-way ANOVA with Tukey's multiple comparisons of the mean of conditions to the mean of the IL4/13/6 control group (p=0.05), n=3 biological replicates across three independent experiments. Error bars represent mean ± SEM.

nanoparticle treatment compared to the untreated IL4/13/6 only group, this shift is not great enough to be considered significant (Fig. 3.7A). Interestingly, observed a significant increase in *Tnf* expression with SA when compared to the stimulated condition (Fig. 3.7B). Lastly, we see no significant shift in *Nos2* throughout our treatment conditions, but we did see an increase after SA treatment when compared to both media only and IL4/13/6 (Fig. 3.7C).

In summary, the constraints of the PCLS model necessitated a strategic focus on the self-assembled nanoparticle platform, which demonstrated the greatest potential for therapeutic development. The inclusion of *Tnf* and *Nos2* in our RT-qPCR analysis revealed that this platform can be used to monitor pro-inflammatory transcriptional programs in lung tissue, indicating its capacity to stimulate immune activation within a complex *ex vivo* environment that has already been pushed towards one that is anti-inflammatory. These findings position the SA nanoparticle system as a promising candidate for targeted immunomodulation in pulmonary disease, warranting deeper mechanistic and translational investigation.

Chapter 4: Examining the effects of RP-182 on anti-inflammatory BMDMs *in vitro*

4.1 Assessing phenotypic changes of anti-inflammatory BMDMs after RP-182 linked polystyrene bead treatment

The second portion of this project included assessing the ability of RP-182 to influence macrophage phenotype. RP-182 is a synthetic peptide first described by Jaynes et. al., where it was found to elicit an antitumour response driven by a pro-inflammatory macrophage program. Additionally, *in vitro* experiments on IL4/13 stimulated BMDMs, increases in pro-inflammatory markers CD86 and secretion of TNF were attributed to the interaction of RP-182 with CD206. We aimed to replicate these observations with the eventual goal of employing RP-182 within a nanoparticle platform with the hope of creating a targeted therapeutic for pulmonary fibrosis.

The first step was to confirm RP-182 recognition and binding by CD206. Using biolayer interferometry, Dr. Ryan Wylie and his student Chuan Yu were able to confirm binding of RP-182 to CD206, which increases with increasing concentration (Supplementary Fig. 2). The next step was to investigate whether the site of peptide conjugation influences immunomodulatory activity. We tested RP-182 formulations grafted onto 0.1 μm PS nanoparticles at either the peptide's C-terminal or N-terminal end. Terminal orientation can affect peptide accessibility, stability, and receptor binding, potentially altering macrophage responses. Both C-linked and N-linked particles were evaluated for their ability to modulate pro-inflammatory and anti-inflammatory surface markers in IL4/13/6 stimulated macrophages.

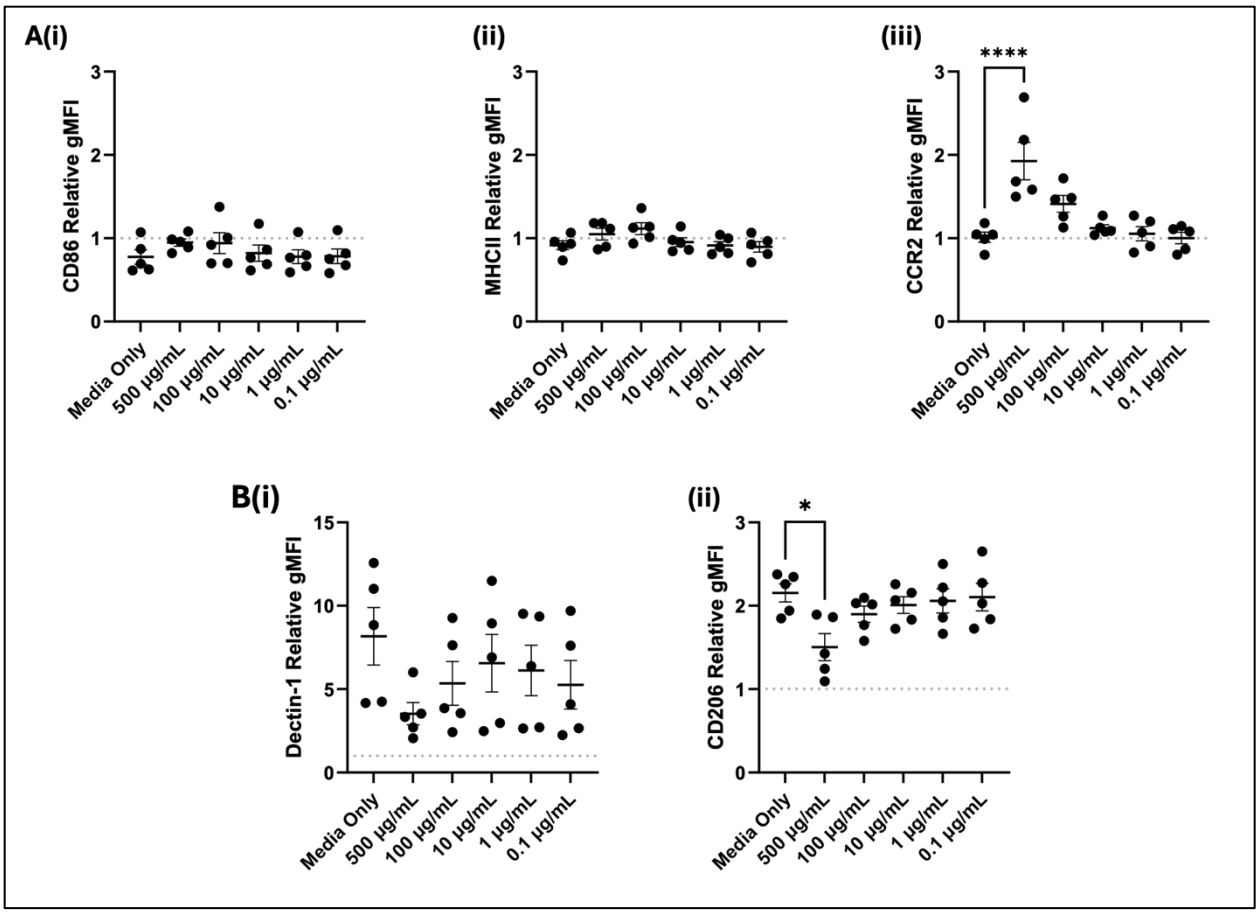

Figure 4.1 C-linked RP-182 nanoparticles decrease anti-inflammatory properties with minimal increases to inflammatory markers. Pro-inflammatory (A) and anti-inflammatory (B) surface marker expression shown as relative geometric mean fluorescent intensity (gMFI) determined by normalizing conditions to their respective unstimulated controls. Statistical significance was analyzed by one-way ANOVA with Tukey's multiple comparisons of the mean of conditions to the mean of the IL4/13/6 control group (p=0.05), n=5 biological replicates across three individual experiments. Error bars represent mean ± SEM, *p < 0.05, ****p<0.0001.

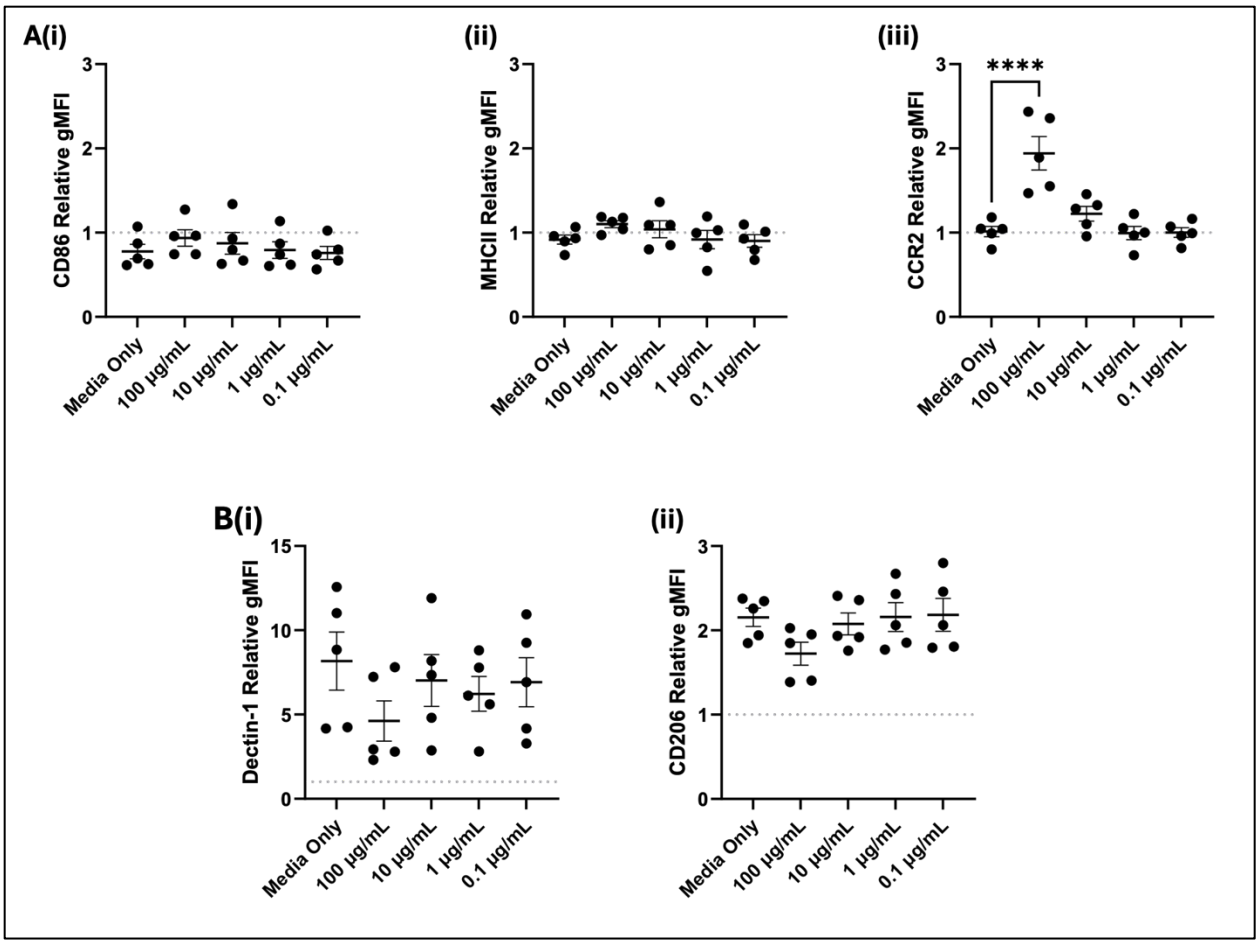

Figure 4.2 N-linked RP-182 nanoparticles do not change BMDM phenotype.

Pro-inflammatory (A) and anti-inflammatory (B) surface marker expression shown as relative geometric mean fluorescent intensity (gMFI) determined by normalizing conditions to their respective unstimulated controls. Statistical significance was analyzed by one-way ANOVA with Tukey's multiple comparisons of the mean of conditions to the mean of the IL4/13/6 control group ($p=0.05$), n=5 biological replicates across three individual experiments. Error bars represent mean ± SEM, ****$p<0.0001$.

Both the C-linked and N-linked particles induced significant increases (2-fold) in CCR2 expression at 500 μg/mL and 100 μg/mL, respectively, compared to IL4/13/6 controls (Fig. 4.1A(iii), 4.2A(iii)). Minimal to no increase in CD86 and CCR2 was observed. When assessing anti-inflammatory markers, C-linked RP-182 particles at 500 μg/mL decreased CD206 expression by approximately 1.3-fold (Fig. 4.1B(ii)), but there were no other significant effects of RP-182 at lower concentrations. Lastly, although not significant, Dectin-1 showed a trend of decreased marker expression with increasing material concentration (Fig. 4.1B(i), 4.2B(i)). It is important to note that the concentration of PS RP-182 materials represented the concentration of the PS bead and not the concentration of RP-182 peptide.

In summary, neither the C-linked nor N-linked PS beads were able to significantly alter BMDM surface marker expression of CD86, MHCII, and Dectin-1. These observations suggest that terminal orientation of the peptide did not influence the bioactivity of RP-182 on BMDMs. Therefore, we decided that RP-182 conjugated to PS via its C-terminus would be used for future experiments.

4.2 Polystyrene drives phenotypic changes in anti-inflammatory BMDMs rather than RP-182

To assess whether concentration of the peptide was important, we tested particles based on peptide concentration ranging from 20 μM – 0.2 μM (Fig. 4.3). Similar to previous findings, a significant increase in CCR2 was observed at the highest concentration tested (Fig. 4.3A(iii)). Interestingly, when treating BMDMs with 20 μM PS RP-182, CD86 surface marker expression increased significantly compared to the untreated control (Fig. 4.3A(i)). Anti-

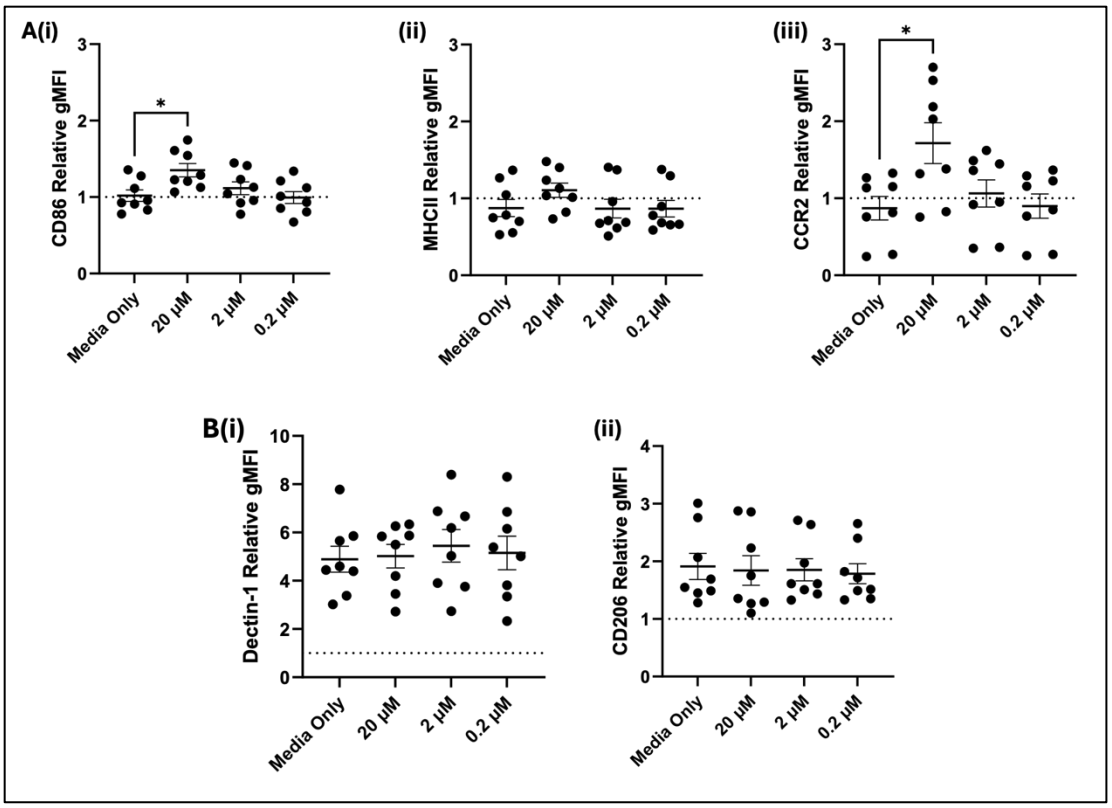

Figure 4.3 PS RP-182 nanoparticles increase pro-inflammatory properties with no impact on anti-inflammatory surface marker expression. Pro-inflammatory (A) and anti-inflammatory (B) surface marker expression shown as relative geometric mean fluorescent intensity (gMFI) determined by normalizing conditions to their respective unstimulated controls. Statistical significance was analyzed by one-way ANOVA with Tukey's multiple comparisons of the mean of conditions to the mean of the IL4/13/6 control group ($p=0.05$), n=8 biological replicates across four individual experiments. Error bars represent mean ± SEM, *$p < 0.05$.

inflammatory markers remained unchanged, contrary to what was seen in Figure 4.1, where PS RP-182 materials were seen to decrease CD206 at 500 μg/mL.

Following testing of the different nanoparticle formulations on their ability to alter macrophage phenotype, we became concerned regarding the increase in inflammatory surface markers such as CD86 and CCR2 induced by PS RP-182 materials (Fig. 4.3). This concern arose from a miscommunication regarding the use of PS as a platform for RP-182. In initial testing, concentration was determined based on the concentration of PS particle and not the bioactive peptide RP-182. This is important as the amount of grafted peptide to PS varied heavily between batches, often complicating direct functional comparison.

These findings drew heightened attention to what was driving changes in anti-inflammatory BMDM phenotype. To evaluate whether the increase in CCR2 and CD86 was being driven by RP-182 or its PS platform, a side-by-side comparison was conducted between PS grafted with RP-182, PS grafted with a scrambled peptide, which contains the same amino acids but in a different sequence to disrupt biological activity, as well as the PS vehicle alone. PS particle concentrations of un-grafted PS were normalized to be equal to the particle count of the PS RP-182 condition. We observed an increase in all three pro-inflammatory surface markers CD86, MHCII, and CCR2 across all three experimental conditions when compared to the untreated control (Fig. 4.4A). Although geometric mean surface expression of the pro-inflammatory markers increased, only PS grafted with scrambled and RP-182 peptides achieved significance (Fig. 4.4A(i)). Additionally, no change was observed in either Dectin-1 or CD206 surface expression (Fig. 4.4B). The results of our previous assays, which suggested RP-182 may not be driving changes in surface marker expression, led us to question the bioactive capacity of our peptide of interest, RP-182.

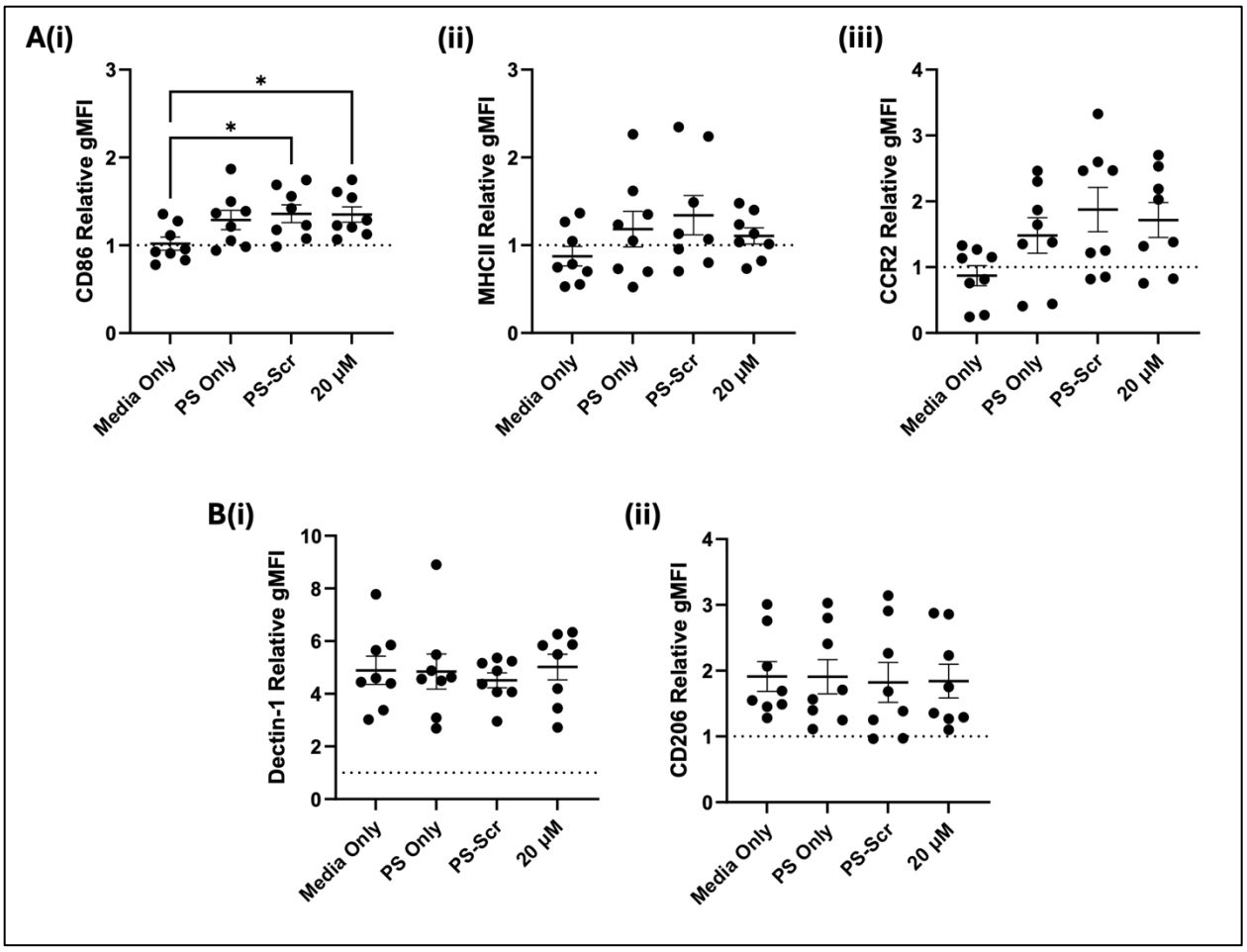

Figure 4.4 The PS vehicle shows similar pro-inflammatory marker expression when compared to other nanoparticle platforms that are conjugated to RP-182 or its scrambled counterpart. Pro-inflammatory (A) and anti-inflammatory (B) surface marker expression shown as relative geometric mean fluorescent intensity (gMFI) determined by normalizing conditions to their respective unstimulated controls. Statistical significance was analyzed by one-way ANOVA with Tukey's multiple comparisons of the mean of conditions to the mean of the IL4/13/6 control group (p=0.05), n=8 biological replicates across four individual experiments. Error bars represent mean ± SEM, *$p < 0.05$.

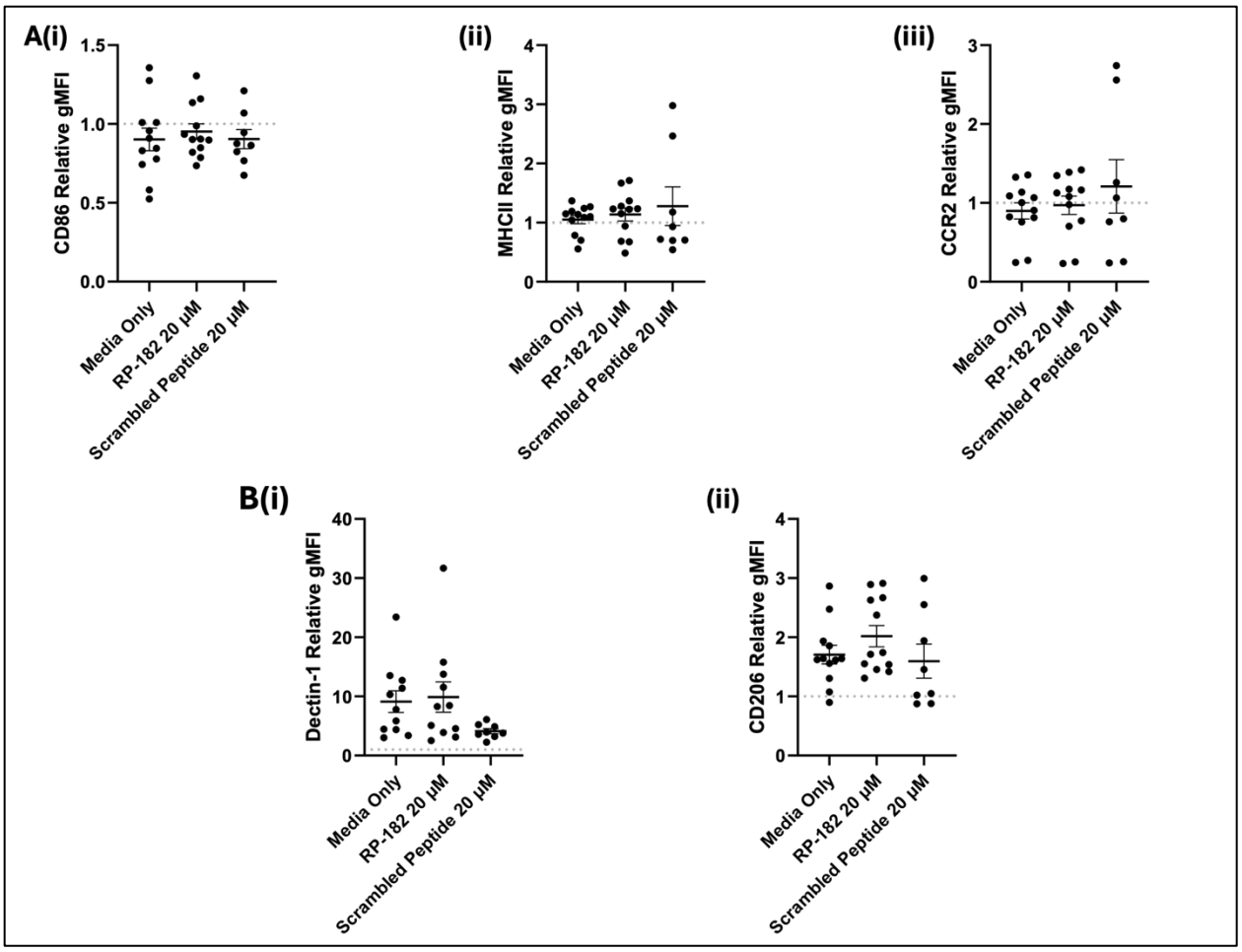

Figure 4.5 RP-182 peptide does not elicit any change in BMDM phenotype.

Pro-inflammatory (A) and anti-inflammatory (B) surface marker expression shown as relative geometric mean fluorescent intensity (gMFI) determined by normalizing conditions to their respective unstimulated controls. Statistical significance was analyzed by one-way ANOVA with Tukey's multiple comparisons of the mean of conditions to the mean of the IL4/13/6 control group (p=0.05), n=12 biological replicates, n=8 for the scrambled peptide. Error bars represent mean ± SEM.

To understand whether the peptide alone induced any changes in macrophage phenotype, we treated cells with 20 μM RP-182 or a scrambled version as described above. No significant shifts in expression of any of the phenotype-specific surface markers were observed (Fig. 4.5). Taken together, these results indicate that the PS vehicle was driving increases in pro-inflammatory surface marker expression. Additionally, the data points to the RP-182 peptide alone being unable to induce a shift away from an anti-inflammatory BMDM phenotype.

Despite the fact that RP-182 showed no ability to induce pro-inflammatory surface marker expression, we found evidence that it interacts and binds to CD206 (Supplementary Fig. 2). We considered whether we might be able to use this system as a drug delivery platform. We conducted uptake assays, which involved fluorescent signal quantification using the Agilent Synergy H1 plate reader and imaging with the EVOS Live Cell Imager to determine internalization of FITC-labelled PS beads and RP-182 conjugates by BMDMs under both stimulatory and control conditions. Our goal was to determine whether BMDMs have preferential uptake of RP-182 grafted PS beads over PS beads lacking the peptide. Additionally, we included a media-only condition as well as an IL4/13/6 stimulated condition where the presence of CD206 on the cell surface was abundant. Our results from the uptake assay, quantifying FITC fluorescence, demonstrated consistent internalization of 0.1 μM PS beads by BMDMs, with no differences between anti-inflammatory or unstimulated naïve BMDMs. Interestingly, this trend continued when RP-182 was conjugated to the PS bead. No differences were observed between activated and inactivated BMDMs. Moreover, uptake of FITC PS was slightly higher than that of RP-182 engrafted beads but failed to result in any significance (Fig. 4.6C, Table 4.1). Similar uptake of PS and the RP-182

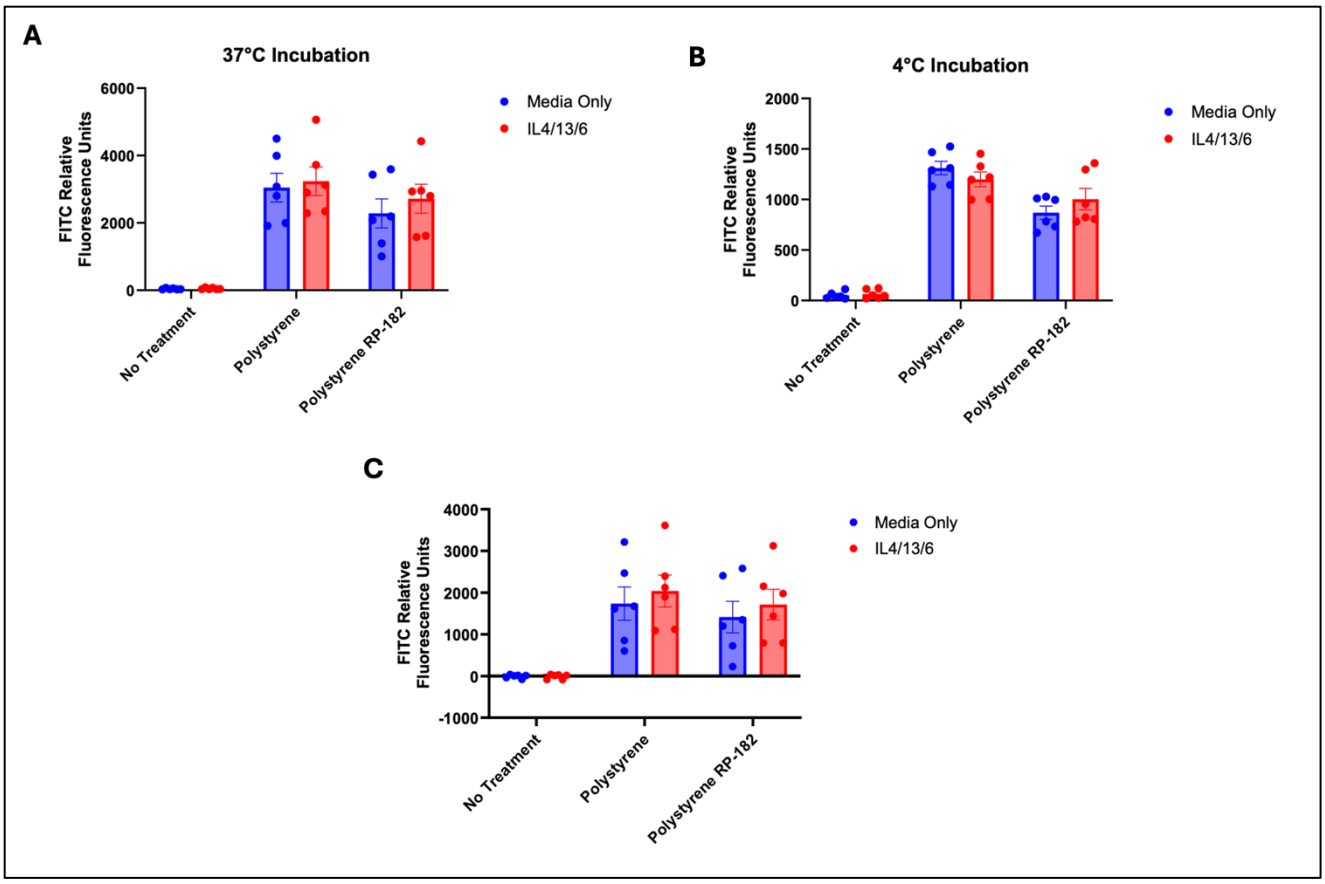

Figure 4.6 Uptake of 0.1 µm PS beads by BMDMs *in vitro* compared to 0.1 µm PS beads with conjugated RP-182 peptide between IL4/13/6 stimulated and unstimulated conditions. BMDMs incubated at 37°C (A) and 4°C (B), and the change in fluorescence between incubation conditions (37°C-4°C) to represent uptake (C). Statistical significance was analyzed by Two-way ANOVA with Šídák's multiple comparisons (p=0.05), n=6 biological replicates across three independent experiments. Error bars represent mean ± SEM,

Table 4.1 Šídák's Multiple Comparisons between conditions after PS/PS-RP182 Treatment of IL4/13/6 stimulated and unstimulated BMDMs

Šídák's Multiple Comparisons	95.00% CI of diff.	t	Adjusted P Value
No Treatment:Media Only vs. No Treatment:IL4/13/6	-1397 to 1408	0.01209	>0.9999
No Treatment:Media Only vs. No Treatment:IL4/13/6	-3148 to -342.8	3.957	0.0064
No Treatment:Media Only vs. PS:IL4/13/6	-3451 to -645.6	4.643	0.001
No Treatment:Media Only vs. PS RP-182:Media Only	-2825 to -20.23	3.225	0.0445
No Treatment:Media Only vs. PS RP-182:IL4/13/6	-3126 to -320.8	3.907	0.0074
No Treatment:IL4/13/6 vs. PS:Media Only	-3153 to -348.1	3.969	0.0062
No Treatment:IL4/13/6 vs. PS:IL4/13/6	-3456 to -650.9	4.655	0.0009
No Treatment:IL4/13/6 vs. PS RP-182:Media Only	-2831 to -25.57	3.238	0.0432
No Treatment:IL4/13/6 vs. PS RP-182:IL4/13/6	-3131 to -326.1	3.919	0.0071
PS:Media Only vs. PS:IL4/13/6	-1705 to 1100	0.6863	>0.9999
PS:Media Only vs. PS RP-182:Media Only	-1080 to 1725	0.7313	>0.9999
PS:Media Only vs. PS RP-182:IL4/13/6	-1381 to 1425	0.04987	>0.9999
PS:IL4/13/6 vs. PS RP-182:Media Only	-777.2 to 2028	1.418	0.935
PS:IL4/13/6 vs. PS RP-182:IL4/13/6	-1078 to 1727	0.7362	>0.9999
PS RP-182:Media Only vs. PS RP-182:IL4/13/6	-1703 to 1102	0.6814	>0.9999

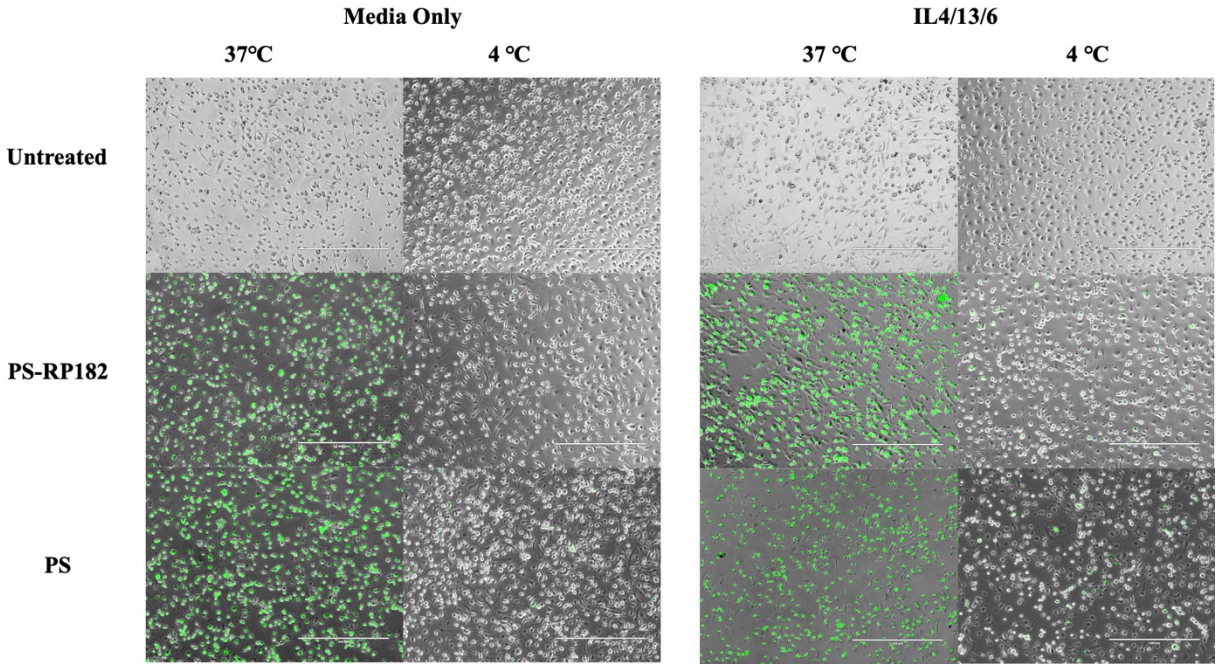

Figure 4.7 EVOS live cell imaging of differences in uptake of 0.1 μm PS beads by BMDMs *in vitro* compared to 0.1 μm PS beads with conjugated RP-182 peptide between IL4/13/6 stimulated and unstimulated conditions. Images illustrate uptake under IL4/13/6-stimulated and unstimulated conditions, with no apparent visual differences in bead internalization between bead type or activation state.

counterpart was seen at both 37°C and 4°C (Fig. 4.6 A-B). This trend was in line with what was seen qualitatively through the EVOS Live Cell Imager, which was used to visualize internalization of FITC conjugated PS, which showed no apparent visual difference in uptake of either PS with or without RP-182 across conditions (Fig. 4.7).

Overall, our findings demonstrated that RP-182 bound to CD206 but did not alter anti-inflammatory BMDM surface marker expression of CD86, MHCII, CCR2, Dectin-1, or CD206, whether administered alone or conjugated to PS nanoparticles. Increases in pro-inflammatory markers CCR2 and CD86 were observed with PS alone, independent of RP-182 presence or peptide orientation. Uptake assays confirmed consistent internalization of PS beads across conditions, with no visual differences observed using live-cell imaging. Lastly, the data indicated that phenotypic changes were driven by the PS vehicle rather than RP-182.

Chapter 5: Discussion

Macrophages are central regulators of lung homeostasis and play a critical role in immune response and wound repair. However, sometimes microenvironmental cues cause these highly plastic immune cells to become drivers of the development and progression of fibrosis within the lung (Lech & Anders, 2013; Wynn & Barron, 2010). More specifically, macrophages are thought to be the primary mediators of fibrosis through their release of profibrotic factors such as TGFβ (Y. Jiang et al., 2024). In addition to their influence over the lung microenvironment, it has been shown that macrophages influence fibrosis progression through bidirectional crosstalk between other cellular players such as fibroblasts and epithelial cells (Froom et al., 2025). Phenotypically, these macrophages are characterized by elevated surface marker receptors such as CD206 and Dectin-1 (Naiel et al., 2023; Pommerolle et al., 2024). Ligand-functionalized nanoparticles may offer a means to either modulate macrophage phenotype directly or selectively deliver therapeutic cargo that modifies macrophage phenotype. In this study, we aimed to induce activation of these receptors with ligand-functionalized nanoparticles. We explored two receptor-directed strategies. The first is β-glucans, which directly engage Dectin-1 to promote phagocytosis and subsequent signalling via CARD9. The second is RP-182, a peptide that induces a conformational change in CD206 (Jaynes et al., 2020; Liu et al., 2015; Naiel et al., 2025), to promote a change from anti- to pro-inflammatory phenotype and function. By incorporating these β-glucans and RP-182 into nanoparticle platforms, our goal was to use a receptor-focused approach to provide a framework for understanding how ligand choice influences both macrophage phenotype and nanoparticle utility in potential antifibrotic therapies.

Our findings with β-glucan nanoparticles highlight the importance of vehicle selection in shaping macrophage phenotype. Consistent with their known interaction with the pattern-recognition receptor Dectin-1 (Mata-Martínez et al., 2022; Reid et al., 2009; Underhill et al., 2005), β-glucan nanoparticles demonstrated a capacity to influence surface marker expression in anti-inflammatory BMDMs. These results suggest that biologically active materials such as β-glucan may provide an inherent advantage as immunomodulatory platforms, as their receptor engagement contributes directly to phenotype modulation. This receptor-driven activity contrasts with what we observed using RP-182 linked PS particles, which lacked intrinsic bioactivity. Instead, the PS vehicle appeared to drive inflammatory changes in surface receptor expression through upregulation of CCR2 predominantly, as well as CD86 and MHCII, irrespective of RP-182 conjugation.

In comparison, RP-182 engrafted PS beads showed limited ability to alter macrophage phenotype beyond what was induced by the PS bead alone. While binding of RP-182 to CD206 was confirmed through BLI at varying concentrations, our data indicates that this interaction failed to translate into any measurable or significant change in BMDM phenotype. Instead, the PS backbone, which was only used as a temporary testing platform, appeared to be the main proponent of pro-inflammatory surface receptor expression. Together, these findings emphasize that the choice of nanoparticle scaffold is a paramount determinant when assessing immunological outcomes. Additionally, RP-182 may be more useful as a targeting ligand engrafted to a biologically inactive or degradable nanoparticle system rather than the primary effector of such a system.

While RP-182 engagement alone may be insufficient to trigger downstream responses, the choice of nanoparticle carrier further complicates interpretation of its bioactivity. Uptake assays confirmed that BMDMs internalized PS nanoparticles efficiently regardless of RP-182 conjugation, but interpretation of the peptide's bioactivity is complicated by the intrinsic properties of the PS vehicle. PS itself has been shown to drive an inflammatory response, upregulating pro-inflammatory surface markers such as CD86, and eliciting TNF and iNOS (W. Jiang et al., 2024; Merkley et al., 2022). Additionally, macrophages readily internalize PS particles within the range of 50 nm to 500 nm, in line with our chosen particle sizes in this study (W. Jiang et al., 2024). This, in turn, creates a strong baseline inflammatory response that could mask any subtle effects induced by RP-182 ligation to CD206. Thus, even if RP-182 engagement produced a moderate effect upon internalization via CD86 upregulation, the inflammatory signature elicited by the PS carrier may overcompensate and obscure the peptide's contribution to such a response. This highlights an important point that the nanoparticle vehicle's immunogenicity can overwhelm or confound detection of ligand-specific effects, underscoring the need for biologically inert or clinically relevant carriers when evaluating receptor-targeting therapeutics.

β-glucans are often viewed as universal Dectin-1 agonists, but their biological effects are highly dependent on their source and structure. The observed outcomes may in part reflect differences in β-glucan structure and therefore its properties, eliciting a lesser response compared to other forms of β-glucan such as curdlan. Large and insoluble, curdlan is a β-glucan derived from the bacteria *Alcaligenes faecalis* and is often used as a pure Dectin-1 agonist that contains no (1,6)-β-linked side chains present in yeast β-glucan. Additionally, both size and solubility play a role in determining the magnitude of a response, where larger insoluble particles induce

greater activation of BMDMs compared to particles that are smaller or more soluble (Elder et al., 2017). More specifically, the particle size of β-glucans themselves can influence the response elicited by Dectin-1 activation, which may be inadvertently hindering our efforts to elicit such a response. As our formulations are soluble and relatively small in size, between roughly 100-200 nm in diameter, these features may be playing an important role in determining the outcome of Dectin-1 activation in response to our β-glucan nanoparticles.

Unlike pattern recognition receptors such as Dectin-1, which contain immunoreceptor tyrosine-kinase based motifs that directly instigate pro-inflammatory programming, CD206 functions primarily as an endocytic mannose receptor. While the exact function of CD206 is still poorly understood, it lacks canonical signalling domains due to its short cytoplasmic tail, resulting in internalized cargo being trafficked to endosomal and lysosomal compartments after receptor engagement of ligands (Allavena et al., 2004; Feinberg et al., 2021). Through this process, the mannose receptor contributes to antigen uptake, clearance of glycosylated ligands, and delivery of materials to compartments where other receptors, such as endocytic TLRs, can be engaged and result in signal induction (Miyake et al., 2019). Thus, RP-182 failing to elicit any pro-inflammatory response in BMDMs isn't completely unsurprising.

Our data has made it clear that platform selection is important to shape macrophage polarization and functional response. One potential alternative worth exploring is the use of poly(oligo(ethylene glycol) methyl ether methacrylate) or POEGMA-based systems. Considered as the next generation replacement for PEGylation, a system used in the mRNA vaccines against SARS-COV-2 (Ju et al., 2023), POEGMA has many ideal properties that make it optimal for our intended use. POEGMA has been widely studied for its biocompatibility, resistance to

nonspecific protein absorption, and ‘stealth’ properties that reduce unwanted immune activation (Ozer et al., 2022; Smeets et al., 2014). Thus, POEGMA scaffolds could provide a more inert platform, allowing RP-182’s effects to be evaluated without confounding background signals from PS-associated immunomodulation. In addition, the chemical versatility of POEGMA permits precise control over particle size, surface charge, and ligand density (Sadowski et al., 2022), which offers an opportunity to optimize RP-182 presentation for targeted uptake via CD206. Thus, incorporating POEGMA particles into future experiments would not only improve the biological relevance of the system but also help assess the translational potential of RP-182 as either a signaling modulator or targeting ligand for macrophage-directed therapies.

Although our results suggest that β-glucan nanoparticles can alter macrophage phenotype by increasing pro-inflammatory receptors MHCII and CCR2, the degree to which these changes are truly Dectin-1-dependent remains unresolved. Dectin-1 engagement is classically associated with Syk phosphorylation, which propagates downstream signalling to drive a pro-inflammatory response (Mata-Martínez et al., 2022; Underhill et al., 2005). To clarify whether the phenotypic changes observed here are mediated by this canonical pathway, future experiments could involve probing for phosphorylated Syk (pSyk) and subsequent NF-κB activity in nanoparticle-treated BMDMs. A straightforward method would be to perform western blots assessing pSyk as well as NF-κB activation. Complementary experiments could involve pre-treating cells with a Dectin-1-blocking antibody, followed by assessment of both particle uptake and downstream signalling, to determine whether an increase in particle uptake is abolished in the absence of receptor engagement. In parallel, it will be important to examine whether crosstalk with other innate immune receptors contributes to the response. It has also been reported that Dectin-1 often interacts synergistically with TLRs. Similar to CD206 engagement, β-glucan internalization

could traffic ligands into endosomal compartments, where TLR engagement could drive the inflammatory response (Li et al., 2019). Assessing nuclear translocation of NF-κB subunits such as p65 by immunofluorescence or probing for TLR-associated markers such as phosphorylated IRF3 could help separate Dectin-1–driven responses from broader PRR signalling. Together, these approaches would provide a more mechanistic picture of how our β-glucan nanoparticles interact with Dectin-1 and shed light on their specificity.

A component of this project aimed to determine whether β-glucans can disrupt the cellular crosstalk involved in fibrosis progression. Current models of fibrosis, including *in vivo* models and *in vitro* cell culture systems, present limitations that complicate mechanistic studies and therapeutic testing. *In vivo* models capture many aspects of the fibrotic process but are time-intensive and costly. Traditional in vitro cultures, while more tractable, oversimplify the disease environment by lacking the complex cellular interactions and extracellular matrix remodelling that define fibrosis. To overcome these challenges, we began with bone marrow–derived macrophages (BMDMs) as a reductionist approach to probe macrophage-specific responses and then transitioned to PCLS to capture multicellular interactions in a more physiologically relevant *ex vivo* setting. *In vitro* or *ex vivo* studies involving IL/4/13/6 stimulation provide a less resource-intensive method to obtain preliminary data on the feasibility and potential of different therapeutic strategies, but do not accurately portray the complex fibrotic response attributed to pulmonary fibrosis. PCLS preserves the multicellular architecture of the lung and maintains essential features of the native extracellular matrix and cellular crosstalk. As PCLS provides a more tissue-relevant model that encompasses the multicellular interactions involved in fibrosis, we used it as a complementary model for our study. We validated our BMDM macrophage polarization using PCLS. Both systems suggest macrophage polarization towards an anti-

inflammatory phenotype as seen through significant increases in *Chil3* in our *ex vivo* model, as well as upregulation of CD206 and Dectin-1 in our *in vitro* model. However, our data showed no changes in the expression of classic fibrosis markers such as *Col1a1, Fn1, Tgfβ,* and *Acta2*. This suggests our PCLS model doesn't effectively induce the early fibrotic response, as seen previously in a fibrotic PCLS model of human lung tissue (Alsafadi et al., 2017). Therefore, we were unable to dissect whether our β-glucan platform can disrupt cellular signalling required to inhibit fibrosis progression, even though there were increases in inflammatory markers such as *Tnf*. Regardless, PCLS slices derived from healthy lungs may not fully recapitulate the altered cellular states, stiffened extracellular matrix, and spatial heterogeneity present in diseased tissue, even after stimulation. Future experiments would benefit from the use of PCLS, but it would be advantageous to incorporate lung slices from well-studied induced fibrosis models, such as bleomycin or adenoviral TGFβ (Lam et al., 2014; Moeller et al., 2008). By employing PCLS tissues from these models, data would more accurately reflect the complex nature of lung fibrosis, as it captures a longer timeframe than what can be recapitulated with lung slices cultured in a dish for a few days.

While this study focuses on macrophages in the fibrotic process, it is also important to recognize that other immune cells express the target receptors Dectin-1 and CD206 under certain conditions. It is recognized that neutrophils and epithelial cells express Dectin-1, and both receptors are present on the cell surface of dendritic cells, although their expression is to a smaller degree than in macrophages (Heyl et al., 2014; Pommerolle et al., 2024; Taylor et al., 2002; Wollenberg et al., 2002). This raises the possibility that nanoparticle engagement with our targeting ligands may not only influence macrophage phenotype but also the behaviour of these other cell types, which would not be identified from BMDM models or by solely focusing on

macrophages within lung slices. While PCLS maintain structural and cellular complexity, they lack systemic inputs such as circulating immune cells, vascular contributions, and long-term remodelling processes that are central to fibrosis progression. *In vivo* studies, such as those using bleomycin-induced pulmonary fibrosis would allow for assessment of how receptor-targeting nanoparticles perform within a fully dynamic immune environment over time. These models would not only provide information on biodistribution and pharmacokinetics but also reveal how macrophage-targeted nanoparticles influence chronic fibrotic pathways, including matrix deposition, immune recruitment, and tissue mechanics. Furthermore, *in vivo* systems would allow for assessment of potential off-target effects. Together, this progression from *in vitro* to *ex vivo* and ultimately *to in vivo* approaches would provide a better framework for evaluating receptor-directed nanoparticles as antifibrotic therapeutics.

Taken together, these findings highlight the dual importance of ligand choice and carrier composition in shaping macrophage responses to nanoparticle-based interventions. A nanoparticle platform with β-glucans modulated BMDM phenotypes through increases in pro-inflammatory surface marker expression, while a nanoparticle platform with RP-182 failed to elicit comparable effects. The poor response of the current RP-182 platform was likely due to both the limited signalling potential of CD206 and the confounding immunogenicity of its engraftment to PS beads. These results emphasize that receptor-targeting strategies must be evaluated within biologically relevant systems and must use biologically inert delivery methods to accurately assess ligand-specific contributions. Looking forward, integrating ligands such as RP-182 into alternative carriers such as POEGMA may provide a clearer understanding of their therapeutic potential while minimizing off-target inflammatory effects. Irrespective of these limitations, assessment of an *ex vivo* PCLS system with cytokine stimulation confirmed

macrophage polarization toward an anti-inflammatory state but revealed limited changes in fibrotic markers. Additionally, pro-inflammatory gene expression of *Tnf* increased after β-glucan nanoparticle treatment, but there was no difference in expression of other classical fibrosis-related genes. By investigating both receptor targeting approaches and delivery vehicle design, this work offers a foundation for developing macrophage-directed nanomedicines that can be translated more effectively into antifibrotic strategies.

Supplementary Data

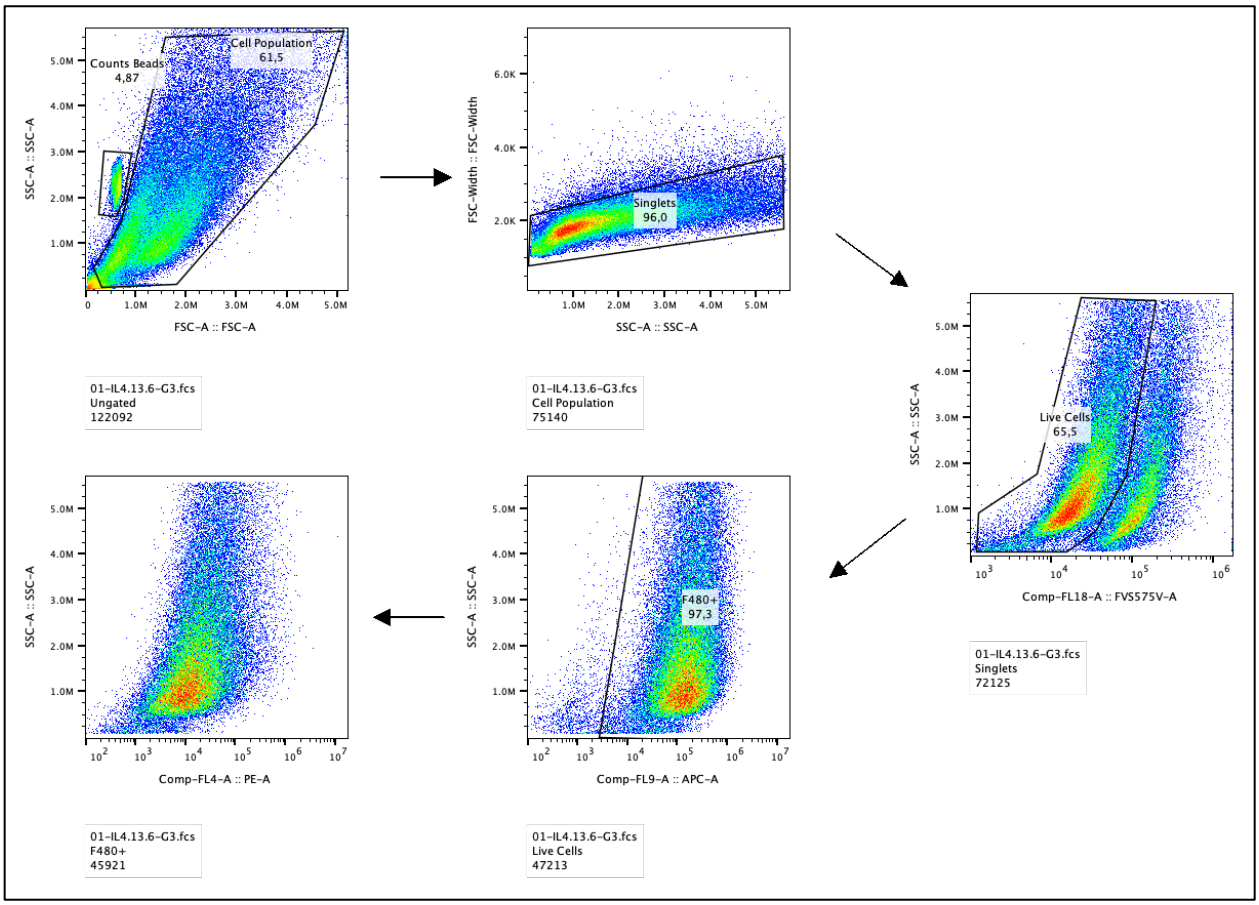

Supplementary Figure 1. Gating strategy used for BMDM Phenotyping

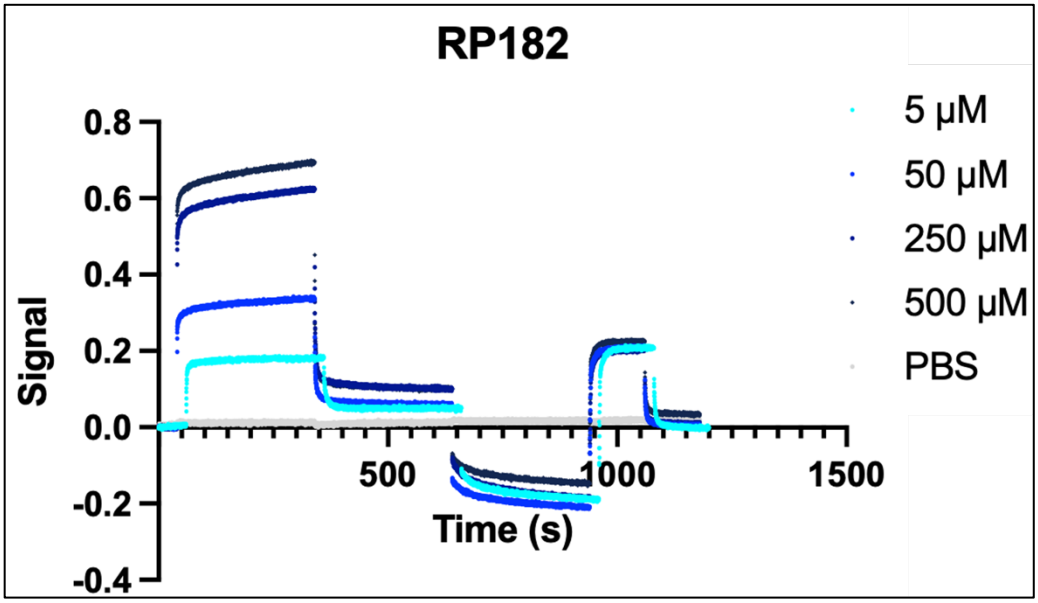

Supplementary Figure 2. Biolayer Interferometry of RP-182 Binding to CD206. An increase in signal strength is representative of RP-182 binding. Decreases seen at times greater than approximately 500 seconds are a result of dissociation of RP-182 from CD206 using an NaCl solution for sensor reloading. BLI assay and data analysis were done by Chuan Yu from Dr. Ryan Wylie's Lab.

References

Aimo, A., Spitaleri, G., Nieri, D., Tavanti, L. M., Meschi, C., Panichella, G., Lupón, J., Pistelli, F., Carrozzi, L., Bayes-Genis, A., & Emdin, M. (2022). Pirfenidone for Idiopathic Pulmonary Fibrosis and Beyond. *Cardiac Failure Review*, *8*, e12. https://doi.org/10.15420/cfr.2021.30

Allavena, P., Chieppa, M., Monti, P., & Piemonti, L. (2004). From Pattern Recognition Receptor to Regulator of Homeostasis: The Double-Faced Macrophage Mannose Receptor. *Critical Reviews in Immunology*, *24*(3), 179–192. https://doi.org/10.1615/CritRevImmunol.v24.i3.20

Alsafadi, H. N., Staab-Weijnitz, C. A., Lehmann, M., Lindner, M., Peschel, B., Königshoff, M., & Wagner, D. E. (2017). An ex vivo model to induce early fibrosis-like changes in human precision-cut lung slices. *American Journal of Physiology-Lung Cellular and Molecular Physiology*, *312*(6), L896–L902. https://doi.org/10.1152/ajplung.00084.2017

Antoniou, K. M., Margaritopoulos, G. A., Tomassetti, S., Bonella, F., Costabel, U., & Poletti, V. (2014). Interstitial lung disease. *European Respiratory Review*, *23*(131), 40–54. https://doi.org/10.1183/09059180.00009113

Arango Duque, G., & Descoteaux, A. (2014). Macrophage Cytokines: Involvement in Immunity and Infectious Diseases. *Frontiers in Immunology*, *5*. https://doi.org/10.3389/fimmu.2014.00491

Arizmendi, N., Puttagunta, L., Chung, K. L., Davidson, C., Rey-Parra, J., Chao, D. V., Thebaud, B., Lacy, P., & Vliagoftis, H. (2014). Rac2 is involved in bleomycin-induced

lung inflammation leading to pulmonary fibrosis. *Respiratory Research*, *15*(1), 71. https://doi.org/10.1186/1465-9921-15-71

Azad, A. K., Rajaram, M. V. S., & Schlesinger, L. S. (2014). Exploitation of the Macrophage Mannose Receptor (CD206) in Infectious Disease Diagnostics and Therapeutics. *Journal of Cytology & Molecular Biology*, *1*(1), 1000003. https://doi.org/10.13188/2325-4653.1000003

Balestro, E., Cocconcelli, E., Tinè, M., Biondini, D., Faccioli, E., Saetta, M., & Rea, F. (2019). Idiopathic Pulmonary Fibrosis and Lung Transplantation: When it is Feasible. *Medicina*, *55*(10), 702. https://doi.org/10.3390/medicina55100702

Bowdish, D. M., & Gordon, S. (2009). Macrophage Function Disorders. In Wiley, *Encyclopedia of Life Sciences* (1st ed.). Wiley. https://doi.org/10.1002/9780470015902.a0002174.pub2

Cheng, Q. J., Farrell, K., Fenn, J., Ma, Z., Makanani, S. K., & Siemsen, J. (2024). Dectin-1 ligands produce distinct training phenotypes in human monocytes through differential activation of signaling networks. *Scientific Reports*, *14*(1), 1454. https://doi.org/10.1038/s41598-024-51620-8

Dancer, R. C. A., Wood, A. M., & Thickett, D. R. (2011). Metalloproteinases in idiopathic pulmonary fibrosis. *European Respiratory Journal*, *38*(6), 1461–1467. https://doi.org/10.1183/09031936.00024711

Dempsey, T. M., Payne, S., Sangaralingham, L., Yao, X., Shah, N. D., & Limper, A. H. (2021). Adoption of the Antifibrotic Medications Pirfenidone and Nintedanib for Patients

with Idiopathic Pulmonary Fibrosis. *Annals of the American Thoracic Society*, *18*(7), 1121–1128. https://doi.org/10.1513/AnnalsATS.202007-901OC

Doolin, M. T., Smith, I. M., & Stroka, K. M. (2021). Fibroblast to myofibroblast transition is enhanced by increased cell density. *Molecular Biology of the Cell*, *32*(22), ar41. https://doi.org/10.1091/mbc.E20-08-0536

Elder, M. J., Webster, S. J., Chee, R., Williams, D. L., Hill Gaston, J. S., & Goodall, J. C. (2017). β-Glucan Size Controls Dectin-1-Mediated Immune Responses in Human Dendritic Cells by Regulating IL-1β Production. *Frontiers in Immunology*, *8*, 791. https://doi.org/10.3389/fimmu.2017.00791

Feinberg, H., Jégouzo, S. A. F., Lasanajak, Y., Smith, D. F., Drickamer, K., Weis, W. I., & Taylor, M. E. (2021). Structural analysis of carbohydrate binding by the macrophage mannose receptor CD206. *Journal of Biological Chemistry*, *296*, 100368. https://doi.org/10.1016/j.jbc.2021.100368

Flaherty, K. R., Fell, C. D., Huggins, J. T., Nunes, H., Sussman, R., Valenzuela, C., Petzinger, U., Stauffer, J. L., Gilberg, F., Bengus, M., & Wijsenbeek, M. (2018). Safety of nintedanib added to pirfenidone treatment for idiopathic pulmonary fibrosis. *European Respiratory Journal*, *52*(2), 1800230. https://doi.org/10.1183/13993003.00230-2018

Froom, Z. S. C. S., Callaghan, N. I., & Davenport Huyer, L. (2025). Cellular crosstalk in fibrosis: Insights into macrophage and fibroblast dynamics. *Journal of Biological Chemistry*, *301*(6), 110203. https://doi.org/10.1016/j.jbc.2025.110203

Goto, Y., Hogg, J. C., Whalen, B., Shih, C.-H., Ishii, H., & Van Eeden, S. F. (2004). Monocyte Recruitment into the Lungs in Pneumococcal Pneumonia. *American Journal of Respiratory Cell and Molecular Biology*, *30*(5), 620–626. https://doi.org/10.1165/rcmb.2003-0312OC

Hall, C. L., Wells, A. R., & Leung, K. P. (2018). Pirfenidone reduces profibrotic responses in human dermal myofibroblasts, in vitro. *Laboratory Investigation*, *98*(5), 640–655. https://doi.org/10.1038/s41374-017-0014-3

Haque, A. S. M. R., Moriyama, M., Kubota, K., Ishiguro, N., Sakamoto, M., Chinju, A., Mochizuki, K., Sakamoto, T., Kaneko, N., Munemura, R., Maehara, T., Tanaka, A., Hayashida, J.-N., Kawano, S., Kiyoshima, T., & Nakamura, S. (2019). CD206+ tumor-associated macrophages promote proliferation and invasion in oral squamous cell carcinoma via EGF production. *Scientific Reports*, *9*(1), 14611. https://doi.org/10.1038/s41598-019-51149-1

Herrera, J., Henke, C. A., & Bitterman, P. B. (2018). Extracellular matrix as a driver of progressive fibrosis. *Journal of Clinical Investigation*, *128*(1), 45–53. https://doi.org/10.1172/JCI93557

Heyl, K. A., Klassert, T. E., Heinrich, A., Müller, M. M., Klaile, E., Dienemann, H., Grünewald, C., Bals, R., Singer, B. B., & Slevogt, H. (2014). Dectin-1 Is Expressed in Human Lung and Mediates the Proinflammatory Immune Response to Nontypeable Haemophilus influenzae. *mBio*, *5*(5), e01492-14. https://doi.org/10.1128/mBio.01492-14

Hu, G., Su, Y., Kang, B. H., Fan, Z., Dong, T., Brown, D. R., Cheah, J., Wittrup, K. D., & Chen, J. (2021). High-throughput phenotypic screen and transcriptional analysis identify

new compounds and targets for macrophage reprogramming. *Nature Communications*, *12*(1), 773. https://doi.org/10.1038/s41467-021-21066-x

Hume, P. S., Gibbings, S. L., Jakubzick, C. V., Tuder, R. M., Curran-Everett, D., Henson, P. M., Smith, B. J., & Janssen, W. J. (2020). Localization of Macrophages in the Human Lung via Design-based Stereology. *American Journal of Respiratory and Critical Care Medicine*, *201*(10), 1209–1217. https://doi.org/10.1164/rccm.201911-2105OC

Ikeda, S., Sekine, A., Baba, T., Kato, T., Katano, T., Tabata, E., Shintani, R., Yamakawa, H., Oda, T., Okuda, R., Kitamura, H., Iwasawa, T., Takemura, T., & Ogura, T. (2022). Randomized phase II study of nintedanib with or without pirfenidone in patients with idiopathic pulmonary fibrosis who experienced disease progression during prior pirfenidone administration. *Medicine*, *101*(22), e29232. https://doi.org/10.1097/MD.0000000000029232

Isshiki, T., Vierhout, M., Naiel, S., Ali, P., Yazdanshenas, P., Kumaran, V., Yang, Z., Dvorkin-Gheva, A., Rullo, A. F., Kolb, M. R. J., & Ask, K. (2023). Therapeutic strategies targeting pro-fibrotic macrophages in interstitial lung disease. *Biochemical Pharmacology*, *211*, 115501. https://doi.org/10.1016/j.bcp.2023.115501

Jaynes, J. M., Sable, R., Ronzetti, M., Bautista, W., Knotts, Z., Abisoye-Ogunniyan, A., Li, D., Calvo, R., Dashnyam, M., Singh, A., Guerin, T., White, J., Ravichandran, S., Kumar, P., Talsania, K., Chen, V., Ghebremedhin, A., Karanam, B., Bin Salam, A., … Rudloff, U. (2020). Mannose receptor (CD206) activation in tumor-associated macrophages enhances adaptive and innate antitumor immune responses. *Science Translational Medicine*, *12*(530), eaax6337. https://doi.org/10.1126/scitranslmed.aax6337

Jiang, W., Liu, Y., Wu, Y., Zhang, L., Zhang, B., Zhou, S., Zhang, P., Xu, T., Wu, M., & Lv, S. (2024). Polystyrene nanoplastics of different particle sizes regulate the polarization of pro-inflammatory macrophages. *Scientific Reports*, *14*(1), 16329. https://doi.org/10.1038/s41598-024-67289-y

Jiang, Y., Cai, R., Huang, Y., Zhu, L., Xiao, L., Wang, C., & Wang, L. (2024). Macrophages in organ fibrosis: From pathogenesis to therapeutic targets. *Cell Death Discovery*, *10*(1), 487. https://doi.org/10.1038/s41420-024-02247-1

Joshi, N., Walter, J. M., & Misharin, A. V. (2018). Alveolar Macrophages. *Cellular Immunology*, *330*, 86–90. https://doi.org/10.1016/j.cellimm.2018.01.005

Joshi, S., Singh, A. R., Wong, S. S., Zulcic, M., Jiang, M., Pardo, A., Selman, M., Hagood, J. S., & Durden, D. L. (2017). Rac2 is required for alternative macrophage activation and bleomycin induced pulmonary fibrosis; a macrophage autonomous phenotype. *PLOS ONE*, *12*(8), e0182851. https://doi.org/10.1371/journal.pone.0182851

Ju, Y., Carreño, J. M., Simon, V., Dawson, K., Krammer, F., & Kent, S. J. (2023). Impact of anti-PEG antibodies induced by SARS-CoV-2 mRNA vaccines. *Nature Reviews Immunology*, *23*(3), 135–136. https://doi.org/10.1038/s41577-022-00825-x

Kalchiem-Dekel, O., Galvin, J., Burke, A., Atamas, S., & Todd, N. (2018). Interstitial Lung Disease and Pulmonary Fibrosis: A Practical Approach for General Medicine Physicians with Focus on the Medical History. *Journal of Clinical Medicine*, *7*(12), 476. https://doi.org/10.3390/jcm7120476

Kendall, R. T., & Feghali-Bostwick, C. A. (2014). Fibroblasts in fibrosis: Novel roles and mediators. *Frontiers in Pharmacology*, *5*. https://doi.org/10.3389/fphar.2014.00123

Kistler, K. D., Nalysnyk, L., Rotella, P., & Esser, D. (2014). Lung transplantation in idiopathic pulmonary fibrosis: A systematic review of the literature. *BMC Pulmonary Medicine*, *14*(1), 139. https://doi.org/10.1186/1471-2466-14-139

Kolosova, I., Nethery, D., & Kern, J. A. (2011). Role of Smad2/3 and p38 MAP kinase in TGF-β1-induced epithelial–mesenchymal transition of pulmonary epithelial cells. *Journal of Cellular Physiology*, *226*(5), 1248–1254. https://doi.org/10.1002/jcp.22448

Koudstaal, T., Funke-Chambour, M., Kreuter, M., Molyneaux, P. L., & Wijsenbeek, M. S. (2023). Pulmonary fibrosis: From pathogenesis to clinical decision-making. *Trends in Molecular Medicine*, *29*(12), 1076–1087. https://doi.org/10.1016/j.molmed.2023.08.010

Kulathu, Y., Grothe, G., & Reth, M. (2009). Autoinhibition and adapter function of Syk. *Immunological Reviews*, *232*(1), 286–299. https://doi.org/10.1111/j.1600-065X.2009.00837.x

Lancaster, L. H., De Andrade, J. A., Zibrak, J. D., Padilla, M. L., Albera, C., Nathan, S. D., Wijsenbeek, M. S., Stauffer, J. L., Kirchgaessler, K.-U., & Costabel, U. (2017). Pirfenidone safety and adverse event management in idiopathic pulmonary fibrosis. *European Respiratory Review*, *26*(146), 170057. https://doi.org/10.1183/16000617.0057-2017

Laskin, D. L., Sunil, V. R., Gardner, C. R., & Laskin, J. D. (2011). Macrophages and Tissue Injury: Agents of Defense or Destruction? *Annual Review of Pharmacology and Toxicology*, *51*(1), 267–288. https://doi.org/10.1146/annurev.pharmtox.010909.105812

Lech, M., & Anders, H.-J. (2013). Macrophages and fibrosis: How resident and infiltrating mononuclear phagocytes orchestrate all phases of tissue injury and repair. *Biochimica et Biophysica Acta (BBA) - Molecular Basis of Disease*, *1832*(7), 989–997. https://doi.org/10.1016/j.bbadis.2012.12.001

Li, M., Hou, Q., Zhong, L., Zhao, Y., & Fu, X. (2021). Macrophage Related Chronic Inflammation in Non-Healing Wounds. *Frontiers in Immunology*, *12*, 681710. https://doi.org/10.3389/fimmu.2021.681710

Li, W., Yan, J., & Yu, Y. (2019). Geometrical reorganization of Dectin-1 and TLR2 on single phagosomes alters their synergistic immune signaling. *Proceedings of the National Academy of Sciences*, *116*(50), 25106–25114. https://doi.org/10.1073/pnas.1909870116

Liao, X., Sharma, N., Kapadia, F., Zhou, G., Lu, Y., Hong, H., Paruchuri, K., Mahabeleshwar, G. H., Dalmas, E., Venteclef, N., Flask, C. A., Kim, J., Doreian, B. W., Lu, K. Q., Kaestner, K. H., Hamik, A., Clément, K., & Jain, M. K. (2011). Krüppel-like factor 4 regulates macrophage polarization. *Journal of Clinical Investigation*, *121*(7), 2736–2749. https://doi.org/10.1172/JCI45444

Liegeois, M., Legrand, C., Desmet, C. J., Marichal, T., & Bureau, F. (2018). The interstitial macrophage: A long-neglected piece in the puzzle of lung immunity. *Cellular Immunology*, *330*, 91–96. https://doi.org/10.1016/j.cellimm.2018.02.001

Liu, M., Luo, F., Ding, C., Albeituni, S., Hu, X., Ma, Y., Cai, Y., McNally, L., Sanders, M. A., Jain, D., Kloecker, G., Bousamra, M., Zhang, H., Higashi, R. M., Lane, A. N., Fan, T. W.-M., & Yan, J. (2015). Dectin-1 Activation by a Natural Product β-Glucan Converts

Immunosuppressive Macrophages into an M1-like Phenotype. *The Journal of Immunology*, *195*(10), 5055–5065. https://doi.org/10.4049/jimmunol.1501158

Malainou, C., Abdin, S. M., Lachmann, N., Matt, U., & Herold, S. (2023). Alveolar macrophages in tissue homeostasis, inflammation, and infection: Evolving concepts of therapeutic targeting. *Journal of Clinical Investigation*, *133*(19), e170501. https://doi.org/10.1172/JCI170501

Mantovani, A., Biswas, S. K., Galdiero, M. R., Sica, A., & Locati, M. (2013). Macrophage plasticity and polarization in tissue repair and remodelling. *The Journal of Pathology*, *229*(2), 176–185. https://doi.org/10.1002/path.4133

Mata-Martínez, P., Bergón-Gutiérrez, M., & Del Fresno, C. (2022). Dectin-1 Signaling Update: New Perspectives for Trained Immunity. *Frontiers in Immunology*, *13*, 812148. https://doi.org/10.3389/fimmu.2022.812148

McQuattie-Pimentel, A. C., Budinger, G. R. S., & Ballinger, M. N. (2018). Monocyte-derived Alveolar Macrophages: The Dark Side of Lung Repair? *American Journal of Respiratory Cell and Molecular Biology*, *58*(1), 5–6. https://doi.org/10.1165/rcmb.2017-0328ED

Merkley, S. D., Moss, H. C., Goodfellow, S. M., Ling, C. L., Meyer-Hagen, J. L., Weaver, J., Campen, M. J., & Castillo, E. F. (2022). Polystyrene microplastics induce an immunometabolic active state in macrophages. *Cell Biology and Toxicology*, *38*(1), 31–41. https://doi.org/10.1007/s10565-021-09616-x

Midgley, A. C., Rogers, M., Hallett, M. B., Clayton, A., Bowen, T., Phillips, A. O., & Steadman, R. (2013). Transforming Growth Factor-β1 (TGF-β1)-stimulated Fibroblast to

Myofibroblast Differentiation Is Mediated by Hyaluronan (HA)-facilitated Epidermal Growth Factor Receptor (EGFR) and CD44 Co-localization in Lipid Rafts. *Journal of Biological Chemistry*, *288*(21), 14824–14838. https://doi.org/10.1074/jbc.M113.451336

Misharin, A. V., Morales-Nebreda, L., Mutlu, G. M., Budinger, G. R. S., & Perlman, H. (2013). Flow Cytometric Analysis of Macrophages and Dendritic Cell Subsets in the Mouse Lung. *American Journal of Respiratory Cell and Molecular Biology*, *49*(4), 503–510. https://doi.org/10.1165/rcmb.2013-0086MA

Miyake, K., Saitoh, S., Sato, R., Shibata, T., Fukui, R., & Murakami, Y. (2019). Endolysosomal compartments as platforms for orchestrating innate immune and metabolic sensors. *Journal of Leukocyte Biology*, *106*(4), 853–862. https://doi.org/10.1002/JLB.MR0119-020R

Naiel, S., Dowdall, N., Zhou, Q., Ali, P., Hayat, A., Vierhout, M., Wong, E. Y., Couto, R., Yépez, B., Seifried, B., Moquin, P., Kolb, M. R., Ask, K., & Hoare, T. (2025). Modulating pro-fibrotic macrophages using yeast beta-glucan microparticles prepared by Pressurized Gas eXpanded liquid (PGX) Technology®. *Biomaterials*, *313*, 122816. https://doi.org/10.1016/j.biomaterials.2024.122816

Naiel, S., Dvorkin-Gheva, A., Vierhout, M., Ayaub, A., Isshiki, T., Ali, P., Revill, S., Reihani, A., Parthasarthy, P., Patel, H., Naqvi, A., Kolb, M., & Ask, K. (2023). Identifying the common denominator: Dectin-1 as a promising marker for macrophage modulation in lung cancer and fibrosis. *Translational Science*, PA4072. https://doi.org/10.1183/13993003.congress-2023.PA4072

Ozer, I., Kelly, G., Gu, R., Li, X., Zakharov, N., Sirohi, P., Nair, S. K., Collier, J. H., Hershfield, M. S., Hucknall, A. M., & Chilkoti, A. (2022). Polyethylene Glycol-Like Brush Polymer Conjugate of a Protein Drug Does Not Induce an Antipolymer Immune Response and Has Enhanced Pharmacokinetics than Its Polyethylene Glycol Counterpart. *Advanced Science*, *9*(11), 2103672. https://doi.org/10.1002/advs.202103672

Perrot, C. Y., Karampitsakos, T., & Herazo-Maya, J. D. (2023). Monocytes and macrophages: Emerging mechanisms and novel therapeutic targets in pulmonary fibrosis. *American Journal of Physiology-Cell Physiology*, *325*(4), C1046–C1057. https://doi.org/10.1152/ajpcell.00302.2023

Plikus, M. V., Wang, X., Sinha, S., Forte, E., Thompson, S. M., Herzog, E. L., Driskell, R. R., Rosenthal, N., Biernaskie, J., & Horsley, V. (2021). Fibroblasts: Origins, definitions, and functions in health and disease. *Cell*, *184*(15), 3852–3872. https://doi.org/10.1016/j.cell.2021.06.024

Pommerolle, L., Beltramo, G., Biziorek, L., Truchi, M., Dias, A. M. M., Dondaine, L., Tanguy, J., Pernet, N., Goncalves, V., Bouchard, A., Monterrat, M., Savary, G., Pottier, N., Ask, K., Kolb, M. R. J., Mari, B., Garrido, C., Collin, B., Bonniaud, P., … Bellaye, P.-S. (2024). $CD206^{+}$ macrophages are relevant non-invasive imaging biomarkers and therapeutic targets in experimental lung fibrosis. *Thorax*, *79*(12), 1124. https://doi.org/10.1136/thorax-2023-221168

Porta, C., Riboldi, E., Ippolito, A., & Sica, A. (2015). Molecular and epigenetic basis of macrophage polarized activation. *Seminars in Immunology*, *27*(4), 237–248. https://doi.org/10.1016/j.smim.2015.10.003

Reid, D. M., Gow, N. A., & Brown, G. D. (2009). Pattern recognition: Recent insights from Dectin-1. *Current Opinion in Immunology*, *21*(1), 30–37. https://doi.org/10.1016/j.coi.2009.01.003

Richeldi, L., Costabel, U., Selman, M., Kim, D. S., Hansell, D. M., Nicholson, A. G., Brown, K. K., Flaherty, K. R., Noble, P. W., Raghu, G., Brun, M., Gupta, A., Juhel, N., Klüglich, M., & Du Bois, R. M. (2011). Efficacy of a Tyrosine Kinase Inhibitor in Idiopathic Pulmonary Fibrosis. *New England Journal of Medicine*, *365*(12), 1079–1087. https://doi.org/10.1056/NEJMoa1103690

Richeldi, L., Du Bois, R. M., Raghu, G., Azuma, A., Brown, K. K., Costabel, U., Cottin, V., Flaherty, K. R., Hansell, D. M., Inoue, Y., Kim, D. S., Kolb, M., Nicholson, A. G., Noble, P. W., Selman, M., Taniguchi, H., Brun, M., Le Maulf, F., Girard, M., … Collard, H. R. (2014). Efficacy and Safety of Nintedanib in Idiopathic Pulmonary Fibrosis. *New England Journal of Medicine*, *370*(22), 2071–2082. https://doi.org/10.1056/NEJMoa1402584

Rőszer, T. (2015). Understanding the Mysterious M2 Macrophage through Activation Markers and Effector Mechanisms. *Mediators of Inflammation*, *2015*, 1–16. https://doi.org/10.1155/2015/816460

Rubins, J. B. (2003). Alveolar Macrophages: Wielding the Double-Edged Sword of Inflammation. *American Journal of Respiratory and Critical Care Medicine*, *167*(2), 103–104. https://doi.org/10.1164/rccm.2210007

Sadowski, L. P., Singh, A., Luo, D. H., Majcher, M. J., Urosev, I., Rothenbroker, M., Kapishon, V., Smeets, N. M. B., & Hoare, T. (2022). Functionalized poly(oligo(lactic acid)

methacrylate)-block-poly(oligo(ethylene glycol) methacrylate) block copolymers: A synthetically tunable analogue to PLA-PEG for fabricating drug-loaded nanoparticles. *European Polymer Journal*, *177*, 111443. https://doi.org/10.1016/j.eurpolymj.2022.111443

Shayhidin, E., Naidoo, A., & Lab, B. (n.d.). *ISOLATION OF MURINE SPINAL BONE MARROW*.

Shi, C., & Pamer, E. G. (2011). Monocyte recruitment during infection and inflammation. *Nature Reviews Immunology*, *11*(11), 762–774. https://doi.org/10.1038/nri3070

Smeets, N. M. B., Bakaic, E., Patenaude, M., & Hoare, T. (2014). Injectable poly(oligoethylene glycol methacrylate)-based hydrogels with tunable phase transition behaviours: Physicochemical and biological responses. *Acta Biomaterialia*, *10*(10), 4143–4155. https://doi.org/10.1016/j.actbio.2014.05.035

Stier, H., Ebbeskotte, V., & Gruenwald, J. (2014). Immune-modulatory effects of dietary Yeast Beta-1,3/1,6-D-glucan. *Nutrition Journal*, *13*(1), 38. https://doi.org/10.1186/1475-2891-13-38

Tanabe, N., McDonough, J. E., Vasilescu, D. M., Ikezoe, K., Verleden, S. E., Xu, F., Wuyts, W. A., Vanaudenaerde, B. M., Colby, T. V., & Hogg, J. C. (2020). Pathology of Idiopathic Pulmonary Fibrosis Assessed by a Combination of Microcomputed Tomography, Histology, and Immunohistochemistry. *The American Journal of Pathology*, *190*(12), 2427–2435. https://doi.org/10.1016/j.ajpath.2020.09.001

Taylor, P. R., Brown, G. D., Reid, D. M., Willment, J. A., Martinez-Pomares, L., Gordon, S., & Wong, S. Y. C. (2002). The β-Glucan Receptor, Dectin-1, Is Predominantly Expressed on the Surface of Cells of the Monocyte/Macrophage and Neutrophil Lineages. *The*

Journal of Immunology, *169*(7), 3876–3882. https://doi.org/10.4049/jimmunol.169.7.3876

T'Jonck, W., Guilliams, M., & Bonnardel, J. (2018). Niche signals and transcription factors involved in tissue-resident macrophage development. *Cellular Immunology*, *330*, 43–53. https://doi.org/10.1016/j.cellimm.2018.02.005

Underhill, D. M., Rossnagle, E., Lowell, C. A., & Simmons, R. M. (2005). Dectin-1 activates Syk tyrosine kinase in a dynamic subset of macrophages for reactive oxygen production. *Blood*, *106*(7), 2543–2550. https://doi.org/10.1182/blood-2005-03-1239

Vancheri, C. (2015). Idiopathic pulmonary fibrosis and cancer: Do they really look similar? *BMC Medicine*, *13*(1), 220. https://doi.org/10.1186/s12916-015-0478-1

Wight, T. N., & Potter-Perigo, S. (2011). The extracellular matrix: An active or passive player in fibrosis? *American Journal of Physiology-Gastrointestinal and Liver Physiology*, *301*(6), G950–G955. https://doi.org/10.1152/ajpgi.00132.2011

Willment, J. A., Lin, H.-H., Reid, D. M., Taylor, P. R., Williams, D. L., Wong, S. Y. C., Gordon, S., & Brown, G. D. (2003). Dectin-1 Expression and Function Are Enhanced on Alternatively Activated and GM-CSF-Treated Macrophages and Are Negatively Regulated by IL-10, Dexamethasone, and Lipopolysaccharide. *The Journal of Immunology*, *171*(9), 4569–4573. https://doi.org/10.4049/jimmunol.171.9.4569

Wollenberg, A., Oppel, T., Schottdorf, E.-M., Günther, S., Moderer, M., & Mommaas, M. (2002). Expression and Function of the Mannose Receptor CD206 on Epidermal Dendritic Cells in Inflammatory Skin Diseases. *Journal of Investigative Dermatology*, *118*(2), 327–334. https://doi.org/10.1046/j.0022-202x.2001.01665.x

Wollin, L., Distler, J. H. W., Redente, E. F., Riches, D. W. H., Stowasser, S., Schlenker-Herceg, R., Maher, T. M., & Kolb, M. (2019). Potential of nintedanib in treatment of progressive fibrosing interstitial lung diseases. *European Respiratory Journal*, *54*(3), 1900161. https://doi.org/10.1183/13993003.00161-2019

Wollin, L., Wex, E., Pautsch, A., Schnapp, G., Hostettler, K. E., Stowasser, S., & Kolb, M. (2015). Mode of action of nintedanib in the treatment of idiopathic pulmonary fibrosis. *European Respiratory Journal*, *45*(5), 1434–1445. https://doi.org/10.1183/09031936.00174914

Wynn, T. (2008). Cellular and molecular mechanisms of fibrosis. *The Journal of Pathology*, *214*(2), 199–210. https://doi.org/10.1002/path.2277

Wynn, T. A., Chawla, A., & Pollard, J. W. (2013). Macrophage biology in development, homeostasis and disease. *Nature*, *496*(7446), 445–455. https://doi.org/10.1038/nature12034

Wynn, T., & Barron, L. (2010). Macrophages: Master Regulators of Inflammation and Fibrosis. *Seminars in Liver Disease*, *30*(03), 245–257. https://doi.org/10.1055/s-0030-1255354

Yamaguchi, M., Hirai, S., Tanaka, Y., Sumi, T., Miyajima, M., Mishina, T., Yamada, G., Otsuka, M., Hasegawa, T., Kojima, T., Niki, T., Watanabe, A., Takahashi, H., & Sakuma, Y. (2017). Fibroblastic foci, covered with alveolar epithelia exhibiting epithelial–mesenchymal transition, destroy alveolar septa by disrupting blood flow in idiopathic pulmonary fibrosis. *Laboratory Investigation*, *97*(3), 232–242. https://doi.org/10.1038/labinvest.2016.135